
Article:
Githumbi, Esther N., Courtney Mustaphi, Colin J. and Marchant, Robert orcid.org/0000-0001-5013-4056 (2021) Late Pleistocene and Holocene Afromontane vegetation and headwater wetland dynamics within the Eastern Mau Forest, Kenya. Journal of Quaternary Science. pp. 239-254. ISSN 0267-8179

https://doi.org/10.1002/jqs.3267

JOURNAL OF QUATERNARY SCIENCE (2021) **36**(2) 239–254 ISSN 0267-8179. DOI: 10.1002/jqs.3267

JQS Journal of Quaternary Science QRA Quaternary Research Association

Late Pleistocene and Holocene Afromontane vegetation and headwater wetland dynamics within the Eastern Mau Forest, Kenya

ESTHER N. GITHUMBI,[1]* COLIN J. COURTNEY MUSTAPHI[2,3] and ROB MARCHANT[4]

[1]Department of Physical Geography and Ecosystem Science, Lund University, Box 117, Lund, 221 00, Sweden
[2]Geoecology, Department of Environmental Sciences, University of Basel, Klingelbergstraße 27, Basel, 4056, Switzerland
[3]Center for Water Infrastructure and Sustainable Energy (W I S E), Futures, Nelson Mandela African Institution of Science & Technology, PO Box 9124, Nelson Mandela, Tengeru, Arusha, Tanzania
[4]York Institute for Tropical Ecosystems, Department of the Environment and Geography, University of York, York, YO10 5NG, UK

Received 14 April 2020; Revised 9 December 2020; Accepted 11 December 2020

ABSTRACT: The Mau Forest Complex is Kenya's largest fragment of Afromontane forest, providing critical ecosystem services, and has been subject to intense land use changes since colonial times. It forms the upper catchment of rivers that drain into major drainage networks, thus supporting the livelihoods of millions of Kenyans and providing important wildlife areas. We present the results of a sedimentological and palynological analysis of a Late Pleistocene–Holocene sediment record of Afromontane forest change from Nyabuiyabui wetland in the Eastern Mau Forest, a highland region that has received limited geological characterization and palaeoecological study. Sedimentology, pollen, charcoal, X-ray fluorescence and radiocarbon data record environmental and ecosystem change over the last ~16 000 cal a BP. The pollen record suggests Afromontane forests characterized the end of the Late Pleistocene to the Holocene with dominant taxa changing from *Apodytes*, *Celtis*, *Dracaena*, *Hagenia* and *Podocarpus* to *Cordia*, *Croton*, *Ficus*, *Juniperus* and *Olea*. The Late Holocene is characterized by a more open Afromontane forest with increased grass and herbaceous cover. Continuous Poaceae, Cyperaceae and Juncaceae vegetation currently cover the wetland and the water level has been decreasing over the recent past. Intensive agroforestry since the 1920s has reduced Afromontane forest cover as introduced taxa have increased (*Pinus*, *Cupressus* and *Eucalyptus*). © 2021 The Authors. *Journal of Quaternary Science* published by John Wiley & Sons Ltd on behalf of Quaternary Research Association

KEYWORDS: afromontane vegetation; Mau Forest; pollen; tropical wetlands; water towers

Introduction

African wetlands are dynamic ecosystems experiencing substantial land use and increasing hydroclimatic variability and stresses to biodiversity (Chapman *et al.*, 2001; MEMR, 2012). Pollen-based analyses that reconstruct changes in past vegetation assemblages and distributions across the highlands of eastern Africa are beginning to characterize the spatiotemporal complexity of montane forests (Livingstone, 1967; Olago *et al.*, 1999; Rucina *et al.*, 2009; Finch and Marchant, 2011; Schüler *et al.*, 2012; Opiyo *et al.*, 2019). Several mountains in Kenya support lake systems that preserve lacustrine sediment archives of palaeovegetation dynamics since the Late Pleistocene (Hamilton, 1982; Marchant *et al.*, 2018; Gil-Romera *et al.*, 2019). Palustrine ecosystems in montane environments have similarly been used to establish environmental histories in equatorial eastern Africa (Hamilton, 1982; Heckmann, 2014; Finch *et al.*, 2017). Among the montane ecosystems of Central Kenya with elevations >3500 m above sea level (asl), such as the Aberdare Range and Mau Escarpment, permanent lake ecosystems are not frequently supported due to steep topography, hydroclimate and sediment infilling. Thus, palustrine, soil, cave and other terrestrial geoarchives are important sources useful for analyses of vegetation change in response to climate, anthropogenic and local-scale mechanisms of environmental change. Longer term insights on ecosystem change from these crucial landscapes that are rich in biodiversity and provide a wide range of ecosystem services can be useful to inform their contemporary management (Gillson and Marchant, 2014).

Kenyan highlands are the headwaters to several large catchments; their forests generate and capture orographic and occult precipitation forming crucial headwater sources for major river systems (Nkako *et al.*, 2005; Cuní-Sanchez *et al.*, 2016; Los *et al.*, 2019). The Mau Forest Complex is one of the five key water towers in Kenya (Nkako *et al.*, 2005; MEMR, 2012). As most of rural sub-Saharan population relies on rain-fed agriculture (Wolff, 2011), and ~70% of Kenyans live in rural areas (Pieterse *et al.*, 2018), understanding the functioning of these headwaters can inform management on the historical evolution and variability of these ecosystems and the ecosystem linkages to the hydrology. Notwithstanding the important roles that mountain ecosystems play with impacts across their wider catchments, high-elevation wetlands receive less ecosystem protection than large lowland wetlands, but are important contributors to biodiversity, landscape diversity, habitat connectivity and social–ecological resilience. This contribution is not just within the highland areas but across the catchment; for example the Mara River flows some 500 km to the south-west through agricultural areas and the Maasai Mara–Serengeti ecosystems and into Lake Victoria and the Nile. The Mau Forest Complex is one of the remaining forest blocks of the western Rift Valley in Kenya, supporting indigenous forests and wildlife and several large communities. The forests have undergone significant change since the late 1800s, conspicuously with the development of industrial forestry during colonial government administration (Klopp, 2012) and ongoing land-use change

*Correspondence: Esther N. Githumbi, as above.
E-mail: esther.githumbi@lnu.se

towards agriculture and continued industrial forestry of exotic tree species (Kenya Gazette Supplement 2012).

Mau forests are divided into seven forest blocks: Eastern Mau Forest is the smallest of these, making the small and isolated remnant indigenous forests the most susceptible to further anthropogenic land-use modifications, climate change effects, ecological disturbances and introduced species (Okeyo-Owuor, 2007; Kinyanjui, 2011; Were *et al.*, 2015). The remaining patches of indigenous forest are protected by legislation for their environmental and ecosystem services and cultural use and heritage (Republic of Kenya, 2016). Much of the lower elevation forests have been converted to agriculture over the past decades (Olang and Musula, 2011; Swart, 2016) with ~25% of the forest converted from AD 1994 to 2009 due to excision and settlement encroachment into the forest (Mwangi *et al.*, 2017). The Government of Kenya recently excised ~353 km^2 of the forest to resettle victims of ethnic clashes as well as members of the Ogiek community previously evicted from the forest. Recent politicking has led to increased illegal settlement, logging and charcoal burning in the forest as a source of income (Nkako *et al.*, 2005; Were *et al.*, 2013). These increased human population pressures on the forests have further fragmented wildlife populations, with subsequent erosion and water distribution issues having consequences for downstream ecosystems and populations (Gichana *et al.*, 2015; Mwangi *et al.*, 2017; Dutton *et al.*, 2018; Mwanake *et al.*, 2019). Neighbouring Mau forest blocks have undergone varying degrees of anthropogenic modifications impacting vegetation biodiversity, soil geochemistry and topsoil seed bank; however, ecological restoration potential remains (Kinjanjui *et al.*, 2013).

The environmental history of the Eastern Mau Forest complex is relatively understudied (Marchant *et al.*, 2018). Early colonial maps described the Mau escarpment as forested but explorers did not penetrate the region before the 20th century. The colonial government established the Mau Forest Reserve (among others) as demands for timber increased with road and railway construction, and exports (Cranworth, 1912). By the AD 1920s, early forest delineations (Troup, 1932) already noted heavy modifications to forests although there was no investigation of the natural history until geological mapping in the 1980s and 1990s (Williams, 1991).

Here we present the first investigation of long-term terrestrial ecosystem change in Eastern Mau documenting how the forest has changed since the Late Pleistocene. After the Last Glacial Maximum, glaciers retreated on the highest mountains of eastern Africa followed by changing elevation vegetation patterns on the mountains (Hamilton, 1982; Van Zinderen Bakker and Coetzee, 1988). As conditions warmed (Loomis *et al.*, 2017), the African Humid Period generally brought higher moisture regimes to the regime from 14 000 to 6000–4000 years BP; with the timing of the transition to relatively drier conditions being time-transgressive and having high spatiotemporal complexity across Africa (Shanahan *et al.*, 2015; Phelps *et al.*, 2020), including highland regions (Street-Perrott *et al.*, 2007). East Africa experienced high precipitation variability characterized by high rainfall in the Early Holocene and increasing, yet highly variable aridity towards the present as evidenced by major drought events (Stager *et al.*, 2003; Verschuren *et al.*, 2009). The effect of increasing CO_2 through the Holocene and varying C_3:C_4 vegetation varied between high- and low-elevation environments (Urban *et al.*, 2015), the last 10 000 BP from the Sacred Lake record on Mount Kenya (Olago *et al.*, 1999) are summarized as dominated by C4 vegetation that reflect the increasing atmospheric CO_2, temperature and precipitation. By the end of the African Humid Period during the Late Holocene, moisture regimes became relatively drier but with high spatiotemporal variability. This was characterized by wetland and lake level variability in lowlands (Verschuren, 2001; Öberg *et al.*, 2012; De Cort *et al.*, 2018), changing montane moisture regimes (Barker *et al.*, 2001, Street-Perrott *et al.*, 2007) and forest pollen assemblages (Rucina *et al.*, 2009; Githumbi *et al.*, 2018a,b; van der Plas *et al.*, 2019; Courtney Mustaphi *et al.*, 2020). Pollen evidence of recent human land use and forest resource use varies between mountains and sites (Ryner *et al.*, 2008; Heckmann *et al.*, 2014; Iles, 2019). For example, in Uganda (Hamilton *et al.*, 1986; Jolly *et al.*, 1998; Lejju, 2009), forest resource use and conversion of land cover have increasingly occurred during in recent centuries (Troup, 1932; Petursson *et al.*, 2013; Gil-Romera *et al.*, 2019; Courtney Mustaphi *et al.*, 2020).

Study region: Kiptunga Forest Block

The Nyabuiyabui wetland (2865 m asl) is located in the Kiptunga Forest Block of the Eastern Mau Forest Block (Fig. 1) that covers an area of 29 000 ha. The surficial geology consists of an extensive thick catena of Early Pleistocene Mau ashes with ferrous basal tuffs (Jennings, 1971; Williams, 1991). Soils are relatively young and productive Udands (Andisols) that contain volcanic tephra. The mantling and subsequent aeolian and hydrological erosion of these deposits have shaped much of the current topography of the mountain ridge and the basin and fluvial channels of the forest and wetland. Kiptunga Forest currently supports populations of birds, reptiles, antelopes, primates and hyenas. The Ogiek community, who historically practised predominantly hunter-gatherer livelihoods, inhabit the region, yet recently, the local populations have increasingly practised pastoralism with cattle, goats and sheep; much of the forested lower elevations have been converted to agriculture (Sang, 2001; Spruyt, 2011).

The Mau forests contain several headwater catchments that flow into the Rift Valley or towards Lake Victoria, most notably through the Mara River, which flows into Maasai Mara and Serengeti. As an orographic precipitation water tower, Mau provides water for rural and urban settlements, pastoral communities and wildlife. The high biodiversity of the Mau forest, the Maasai Mara National Reserve and Serengeti National Park have led to the designation of the three regions as Important Bird Areas. They are also habitat to high numbers of large game and host both indigenous and threatened animals such as the bongo and the yellow-backed duiker, the golden cat, the leopard and the African elephant (Nkako *et al.*, 2005).

Scattered minor pockets of remnant indigenous broadleaf forests include *Croton*, *Dombeya*, *Hagenia*, *Juniperus*, *Olea* spp., *Podocarpus* and *Prunus*. The Maasai Mau block is entirely indigenous comprising a *Juniperus–Podocarpus* mosaic interspersed with indigenous vegetation glades (Nkako *et al.*, 2005). The highly valued indigenous timber species are *Albizia gummifera*, *Olea capensis*, *Juniperus procera*, *Polyscias kikuyuensis*, *Podocarpus* spp., *Pouteria* spp., *Prunus africana* and *Strombosia* spp. The major land cover classes (forests–shrublands, grasslands, croplands, urban areas, barren land cover and open water) have undergone tremendous changes over the last few decades with a decrease in Afromontane vegetation cover accompanied by an increase in agricultural and fragmented land and modifications to wetlands (MEMR, 2012; Were *et al.*, 2013). In addition to broad-scale land-use transition there is quite common selective harvesting of tree species, and collection of poles, non-timber forest products and firewood. Few patches of indigenous forest remain due to intensive tree replanting–harvesting cycles of introduced tree species partitioned into plantation plots (Sanya, 2008).

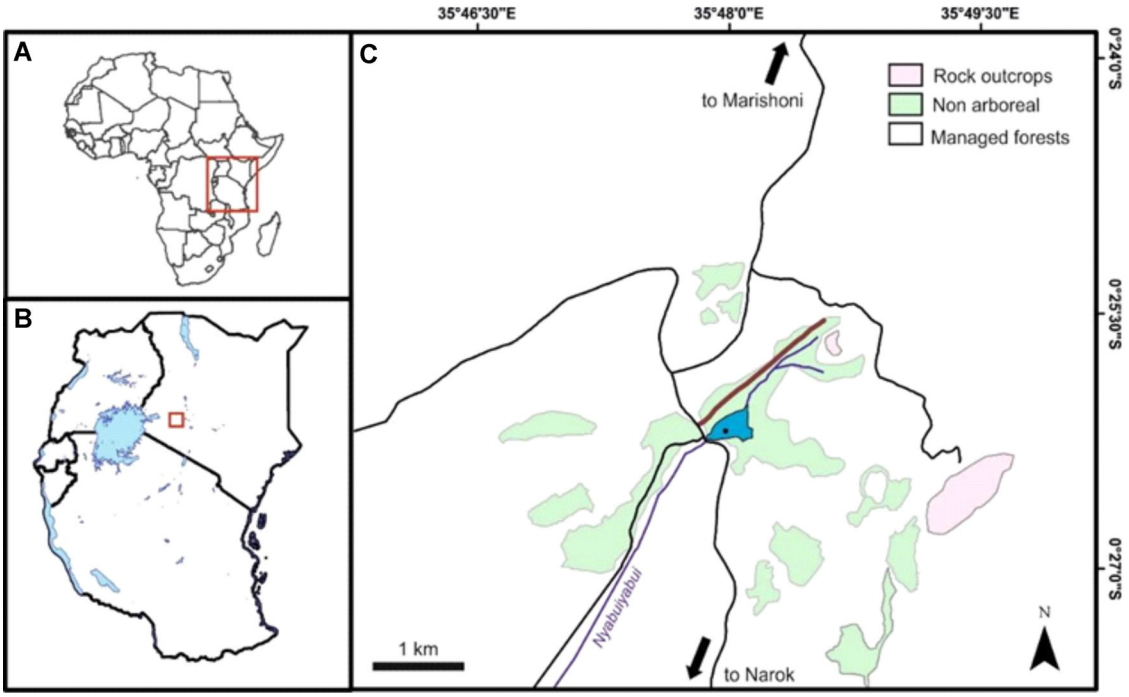

Figure 1. Location of the Nyabuiyabui study site within (A) Africa, (B) East Africa and (C) Kiptunga forest block, Kenya. Shown are the extent of the Cyperaceae–Poaceae-dominated wetland (shown in blue) with the outflow tributary flowing south-west, a fire break cut line (red line) to protect the forests from fire, and coring location (black circle; 0°26 ′11.28 ″S, 35°47′58.74″ E; 2920 m asl). [Color figure can be viewed at wileyonlinelibrary.com]

Agroforestry species include indigenous *Juniperus procera*, and introduced taxa include *Cupressus lusitanica*, *Eucalyptus maculata* (syn. *Corymbia maculata*) and *Pinus patula*.

Study site: Nyabuiyabui wetland

The *Nyabuiyabui* hydronym is an Ogiek word meaning 'spongy' (Spruyt, 2011) or 'marshy', and may support a floating vegetation mat during wetter intervals. Nyabuiyabui wetland (Fig. 1) covers an area of 122 ha within the Kiptunga Forest Block. The current waterlogged/open water area extends to about 6 ha although water levels vary in response to local hydroclimatic conditions. Nyabuiyabui has minor ephemeral inflows and a single outflow to the south-west that forms a tributary of the Mara River network. The wetland is shallow with observed water depths at the centre of the basin well below 50 cm during March–April 2014 and lower still (<20 cm) during April 2015. Anecdotal discussions with local people suggested that the water level has been decreasing during the remembered past and that there was open water within the wetland and a flowing outflow channel under the road bridge before 1972.

There is evidence of recent anthropogenic modifications of the wetland, namely infrastructure, grazing and introduced species. Logging-access roads have been constructed around the wetland as well as a concrete bridge over the outlet. A cut line running along the west margin to stop grass fires from threatening the forests, a now unused pumping station that supplied water to the Kiptunga Forest Station buildings and former tree nursery uphill remain near the wetland shore immediately east of the bridge. The presence of the pump house also supports the plausibility of higher water levels during the early to mid-20th century. Cattle graze along the wetland margin and impact the hummocky ground and morphology of the Poaceae–Cyperaceae–Juncaceae tussocks. The wetland is surrounded by small patches of indigenous forest and monoculture tree plots of varying ages with planting dates from AD 1935 to 2006 and predominantly during the 1960s (Sanya, 2008; Courtney Mustaphi *et al.*, 2016). As of 2015, plantation plots of *Cupressus lusitanica* were the most predominant in the watershed surrounding the wetland. The closest archaeological records are human and animal remains from an excavated burial cave, north-east of the wetland but significant forestland use could not be determined from the finds. The finds were ascribed to the Late Stone Age due to their similarity to finds from that period (Faugust and Sutton, 1966; Merrick and Monaghan, 1984).

Methods

Field methods

In 2014, a suitable coring site was determined by probing the sediments with fibreglass rods along transects to locate the maximum accumulation. A 537-cm core was recovered from 0°26 ′11.28 ″S, 35°47′58.74″E, 2920 m asl near the wetland centre using a hand pushed hemicylindrical Russian corer 5 cm in diameter (Fig. 1). Sediment cores were collected in 50-cm drives with 10-cm overlapped sections from parallel coring holes. Cores were transferred to longitudinally split PVC tubes, wrapped in plastic wrap and aluminium foil, shipped to the University of York, UK, and refrigerated at 4 °C.

Laboratory analysis

Six bulk sediment subsamples and three sieved and picked organic matter (plant material) samples were accelerator mass spectrometry (AMS) radiocarbon dated at Queen's University Belfast ^{14}CHRONO laboratory, UK; Scottish Universities Environmental Research Centre (SUERC), Glasgow, UK; or DirectAMS, Bothell, USA. The IntCal13 curve (Reimer *et al.*, 2013) was used to calibrate the dates and an age–depth model was developed using a BACON R script with default settings (Blaauw, 2010; Blaauw and Christen, 2011; R Development Core Team, 2017). Several iterations of potential age–depth models were run to explore the potential ranges for bounds to

stratigraphic zonations and to extrapolate a basal date. More confidence was given to sieved plant material (mostly grass charcoal fragments) that frequently provide narrower dating uncertainties over bulk sediment AMS radiocarbon dates (Rey *et al.*, 2019) because of the relatively short growth time of above-ground grassy fuel.

Loss-on-ignition (LOI) and particle-size distribution analyses were carried out to characterize the sediments: organic matter content, carbonate content and mean clastic particle size every 5 cm down core. LOI analysis involved weighing the wet samples and then again after drying at 105, 550 and 950 °C (for 24, 5 and 3 h, respectively) to calculate the dry weight, organic matter and carbonate contents, respectively (Heiri *et al.*, 2001). Particle-size distribution analysis was carried out using the Malvern laser granulometer (MEH/MJG180914). The procedure involved pretreating 1-cm^3 wet sediment subsamples with 30% hydrogen peroxide in a hot water bath to digest organic matter and reduce particle aggregation (Syvitski, 1991). If the subsample contained <3.5% organic matter, the hydrogen peroxide treatment was skipped. At a pump speed of 1500, 1–2 g of sample was added until laser obscuration in the measurement column was 4%. The granulometer repeated three measurements and calculated an average result (Malvern Instruments Ltd, 2007).

The cores were scanned using a Cox Analytical Systems ITRAX core scanner at the Department of Geography and Earth Sciences, Aberystwyth University, UK. The ITRAX core scanner collected optical imagery of the core face using an RGB digital camera, and measured magnetic susceptibility using a Bartington MS2E sensor at 1-cm intervals and air-corrected between measurements. Magnetic susceptibility is the degree of magnetization in response to a magnetic field measured in intensity values that are dimensionless units (χ). The X-ray fluorescence (XRF) results represent a semiquantitative measurement of elemental composition in kcps (thousands of counts per second) of the sediment matrix. In total, 22 elements were examined at 0.05-cm intervals through XRF with a 3-kW water-cooled molybdenum anode X-ray tube (60 kV, 35 mA, 200-ms exposure). The results are influenced by potential X-ray absorption and/or scattering across the core due to variability in water content, particle size distributions, mineralogy and surface roughness of cleaned core face (Croudace *et al.*, 2006).

Subsamples of 1 cm^3 of sediment were extracted at 1-cm intervals from the wet core face for macroscopic charcoal analysis. This was soaked in sodium hexametaphosphate solution to disaggregate the organic material and clay particles (Bamber, 1982). A drop of hydrogen peroxide whitened non-charcoal organic matter (Schlachter and Horn, 2010; Whitlock *et al.*, 2010). Samples were gently wet sieved through a 125-μm mesh, and the retained charcoal pieces were identified by visual inspection and probed with a metal needle (Hawthorne and Mitchell, 2016; Vachula, 2019) and tallied under a Zeiss Axio Zoom V16 microscope at magnifications of 10–40×. Counts were converted to charcoal concentration values (number of particles per unit volume, pieces cm^{-3}).

A 1-cm^3 subsample was obtained every 10 cm for pollen and spore analysis following sequential chemical digestion steps using 10% HCl, 10% KOH and acetolysis (Faegri and Iversen, 1950, 1989; Erdtman, 1960). Heavy liquid separation using sodium polytungstate ($3NaWO_4.9WO_3.H_2O$ with relative density = 2) was carried out after acetolysis (Neumann *et al.*, 2010; Quick, 2013; Colombaroli *et al.*, 2018). One tablet of the acetolysed exotic marker *Lycopodium* spores ($n = 9666$, $\sigma = 212$ spores per tablet; University of Lund batch no. 3682) was added before pollen preparation to aid in calculation of absolute concentrations (Stockmarr, 1971; Bonny, 1972).

The data were analysed using: Rbacon package version 2.3.9.1 to develop the age–depth model using Bayesian approaches. Dates identified as outliers in the initial BACON run (default settings) were the bulk sediment samples. A study published in 2018 looking at the impact of model choice, dating density and quality on chronologies found that using BACON outliers were found to have little to no impact on model precision (Blaauw *et al.*, 2018). Rioja version 0.9-21 (Juggins, 2020) was used to run the hierarchical constrained clustering – CONISS (ITRAX, charcoal and pollen), calculate the statistically significant number of assemblage zones (Bennett, 1996) and C2 for stratigraphic plots (Juggins, 2003). CONISS analysis was carried out on the complete pollen dataset but for ease of view we present the dominant taxa in each grouping in the text and the complete pollen diagram in the Supporting Information.

Data accessibility

All data generated from this study will be openly available via the African Pollen Database (Vincens *et al.*, 2007), a constituent of the Neotoma Paleoecology Database and data repository (Grimm *et al.*, 2018; Williams *et al.*, 2018).

Results

General lithology description and geochronology

Six lithological units were identifiable from the 537-cm sediment core that was mainly dark organic-rich silty sediment. The top 8 cm comprised organic-rich detritus, mainly plant roots. This changed into a layer of dark grey clayey silt that extended until 124 cm (between 84 and 124 cm there is an increase in the coarse sand fraction). From 124 to 385 cm the sediment changes to a dark brown silt layer (>80%) with grey/black laminations between 224 and 274 cm. Starting with a thick black layer at 386 cm, the sediment becomes a darker brown sandy silt until 474 cm. From 475 cm to the bottom, the sediment changes back to a dark grey sandy silt with light coloured laminations and concretions at depths with increasing sand. The transitions in sediment colour and type along the core are rapid and distinct except in the bottom 1 m where laminations are visible.

Nine radiocarbon dates were used in BACON (Blaauw, 2010) to develop a plausible age–depth model (Fig. 2; Table 1). The Bayesian model recognizes four ages as outliers: 2449 ± 35 cal a BP at 50–51 cm, 10 721 ± 47 cal a BP at 100–101 cm and 14 424 ± 45 cal a BP at 384–853 cm are older than the dates below them, and 13 963 ± 60 cal a BP at 315–316 cm is younger than the dates above it. Due to the relatively low number of available dates to construct a robust age–depth mode,l we use the most parsimonious suite of dates based on macrofossils and the most likely date sequence (Fig. 2). In addition, the palaeoenvironmental changes are primarily discussed within depth boundaries and the ages discussed within broad time intervals/stratigraphic stages (Walker *et al.*, 2019), i.e. Late Pleistocene to Early Holocene (538–~240 cm), the early and Middle Holocene (240–100 cm) and the Late Holocene from 100 cm to the top (present).

Sedimentology

The sedimentology is highly variable along the core (Fig. 3). LOI results show that the sediment bulk density ranged between 0.1 and 3.2 g cm^{-3} with an average of ~1 g cm^{-3} and standard deviation (SD) of ~0.5, organic matter ranged

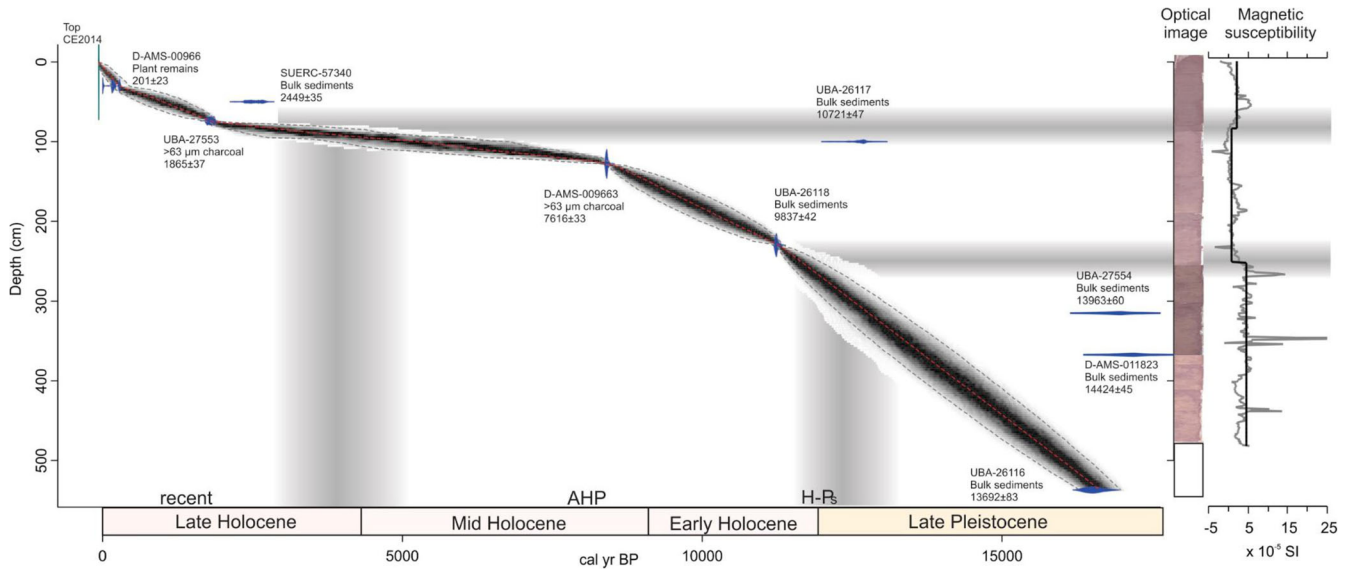

Figure 2. Age–depth model developed from nine radiocarbon dates using the Rbacon package (Blaauw and Christen, 2011) and weighted mean (red dashed line) and the 95% confidence interval of ~8 million random walks through the calibrated radiocarbon age probability densities (Reimer *et al.*, 2013) (low and upper limit = grey line). Optical image and magnetic susceptibility measured during ITRAX core scanning (see Methods). Down-core zonations were defined using the magnetic susceptibility, ITRAX and pollen assemblage zones, showing broad agreement in major changes in the sediment stratigraphy. Geological stages of the Quaternary (Walker *et al.*, 2019) are shown below. AHP, African Humid Period (Demenocal *et al.*, 2000); H, Holocene; Ps, Pleistocene. Note that there was no optical image or magnetic susceptibility data for the deepest section of core from 450–537 cm. [Color figure can be viewed at wileyonlinelibrary.com]

from 0 to 100% with an average of ~21% and SD of ~18, while the carbonate content ranged between 0 and 40% with an average of ~6% and SD of ~7.

The sediment is composed of organic material mixed with varying amounts of silt, sand and clay (Fig. 3). The silt content is highest with an average of 72.44 ± 1.13% (ranging from ~34 to 86%), followed by sand with an average of 17.84 ± 1.13% (ranging between 2 and ~63%) and finally clay with an average of 9.63 ± 0.39% (ranging between ~1.6 and 19%). The sand component is most variable throughout the sediment core. A stratigraphically constrained cluster analysis highlights three distinct zones. From the bottom of the core to 370 cm covering the end of the Pleistocene, the clay content ranges between ~3 and 15%, silt between 52 and 81%, and highest variance is in the sand content between 10 and 55%. Clay content is the lowest, averaging ~7% followed by ~67% silt and ~26% sand; this zone can be described as a sandy silt. The second zone from 365 to 120 cm, covering the end of the Pleistocene and Early Holocene, shows an increase in clay and silt percentages to ~11 and ~80%, respectively, and a decrease in the sand content to ~9%. The clay content ranges between 5 and ~18%, silt ~57- to ~86%, and sand 2 to ~33%; this zone can be described as a clayey silt. The top of the record from 115 cm to the top of the core consists of a sandy silt-like bottom section where the average clay is ~11%, silt is ~65% and sand is ~26%. The clay content remains at ~11% while the silt decreases from 80 to 65% and the sand increases from ~9 to ~26%.

Bulk density is higher in the bottom half of the core (530 to ~260 cm) during what would be the Late Pleistocene. It gradually decreases, and between 155 and 75 cm (Early and Middle Holocene) it averages 0.5 g cm^{-3}. From 70 cm to the top of the core (Late Holocene), average bulk density increases back up to ~1 g cm^{-3}. The organic matter and carbonate content are lowest in the lower half of the record (Late Pleistocene) at ~12 and 4%, respectively. This increases to 16 and 10% between 260 and 160 cm around the Late Pleistocene/Early Holocene interval. The section from 155 to 75 cm (Early to Late Holocene period) has the highest increase in organic matter at an average of 40%, while the carbonate content decreases to 6%. The top of the record (from 100 to 0 cm), representing the Late Holocene, has organic matter and carbonate content of ~35 and ~6%, respectively.

Table 1. Radiocarbon dating results from the 537-cm-long core collected in 2014.

Depth (cm)	Age (^{14}C a BP)	pMC (%)	Material	Laboratory code
0				Top of core
30–31	201 ± 23	97.53 ± 0.28	Plant remains	D-AMS-009664
50–51*	2449 ± 35	73.72 ± 0.32	Bulk sediment	SUERC-57340
74–76	1865 ± 37	79.37 ± 0.13	>63 µm charcoal	UBA-27553
100–101*	10 721 ± 47	26.33 ± 0.15	Bulk sediment	UBA-26117
128–129	7616 ± 33	38.75 ± 0.16	>63 µm plant remains	D-AMS-009663
230–231	9837 ± 42	29.39 ± 0.15	Bulk sediment	UBA-26118
315–316*	13 963 ± 60	17.58 ± 13	Bulk sediment	UBA-27554
384–385*	14 424 ± 45	16.602 ± 0.094	Bulk sediment	D-AMS 011823
536–537	13 692 ± 83	18.19 ± 0.19	Bulk sediment	UBA-26116

Radiocarbon ages are presented with 1σ measurement error. pMC, per cent modern carbon with 1σ measurement error.
*Dates identified as outliers in the age–depth model.

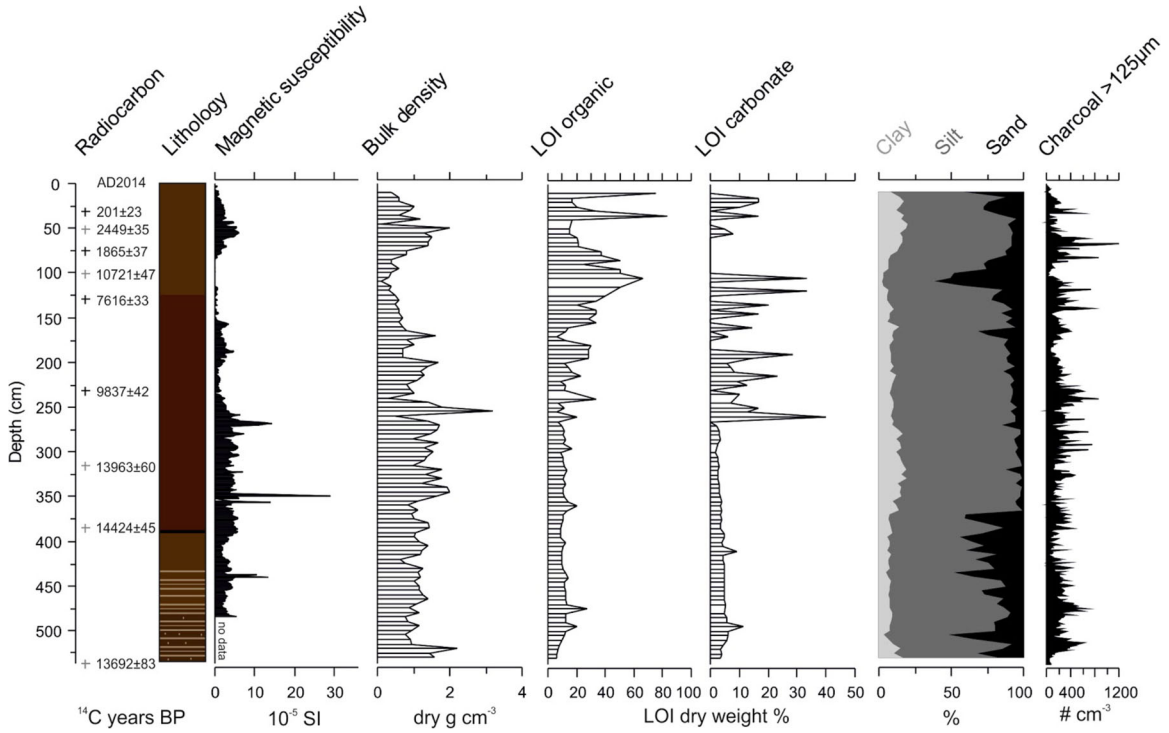

Figure 3. Characterization of the sediments from a 537-cm-long core collected from Nyabuiyabui. Uncalibrated radiocarbon ages, general lithology, dry bulk density, and organic and carbonate content estimates from loss-on-ignition analysis. Laser particle size determinations presented as relative per cent of clay (<4 μm), silt (4–63 μm) and sand fractions (63–2000 μm), and charcoal concentrations are shown. [Color figure can be viewed at wileyonlinelibrary.com]

Elemental profile and magnetic susceptibility (χ)

The ITRAX core scanner was set to detect counts for 22 elements (Fig. 4; Table 2); Ni and I were not included in further data analyses because both occurred at very low concentrations and had a limited stratigraphic pattern (Githumbi, 2017). Magnetic susceptibility readings expressed as χ, or volume susceptibility, represent the ratio of magnetization in samples (per unit volume) to the magnetic field created by the sensor, and are dimensionless with a scale of 10^{-5} SI units (Burrows *et al.*, 2016).

Elemental composition was dominated by Fe (average 85.25 cps), Zr (6.5 cps) and Y (2.6 cps). Rb (1.3 cps) and Ti (1.2 cps) are the only other elements with average cps values >1 through the sediment core. Magnetic susceptibility (χ) varied through the sediment record between −4.14 and 70.89×10^{-5} SI with an average of 2.97. A stratigraphically constrained cluster analysis divided the elemental composition record into three significant zones labelled ITRAX1, ITRAX2 and ITRAX3 (Fig. 4).

ITRAX1 extends from 484 to 260 cm covering the Late Pleistocene to the Early Holocene. Fe (ranging from 82.46 to 92.82 cps), Zr (2.67 to 7.14 cps), Y (1.03 to 3.24 cps), Rb (0.91 to 2.33 cps), Mn (0.23 to 7.69, with an average of 0.9 cps) and Ti (0.79 to 1.59, with an average of 1.2 cps) had the highest average counts in this zone. Magnetic susceptibility averaged 4.47. In the next zone, ITRAX2 (from 260 to 127 cm), covering part of the early to mid-Holocene, the same elements still dominated with a slight increase in Zr, Y and Rb, while Ti and Mn decreased. Mn decreases from ~1.6 to 0.6 cps. The top zone, ITRAX3, extends from 127 cm to the core top and includes the rest of the Holocene to the present. Between 113 and 100 cm, all the elements experience a spike except Ti, K and Fe, which decrease. In this zone, all the elements exhibit an increased trend in counts towards the top except K, Rb and Sr (Fig. 4). Pb shows the greatest increase from 0.022 (ITRAX3), 0.031 (ITRAX2) to 0.21 in ITRAX1, almost a 10-fold increase. Hg shows a similarly large increase in the uppermost sediment samples.

Charcoal record (125 μm)

Charcoal concentration fluctuated from the Late Pleistocene to present at 0–1198 pieces cm^{-3} with a mean of 217 pieces cm^{-3}. Charcoal varies throughout the record and the CONISS analysis identifies three significant zones. The bottom of the record to 307 cm is the first zone, CHAR3, and covers the Late Pleistocene period, the second zone is from 306 to 105 cm and is divided into two subzones CHAR2B and CHAR2A, and the top zone starts at 104 cm and covers the Late Holocene.

CHAR3, covering the Late Pleistocene and Early Holocene transition, experiences fluctuations in charcoal concentration; minimum, maximum and mean charcoal concentration values are 25, 863 and 230 pieces cm^{-3}. The mean concentration is higher than the mean throughout the whole record. These values are lower in the next zone, CHAR2B, to 14, 727 and 205 pieces cm^{-3}, respectively. In CHAR2A there is a significant increase in the charcoal concentration, with minimum, maximum and mean values of 16, 1198 and 238 pieces cm^{-3}, respectively. The topmost zone is CHAR1 where charcoal concentration decreases significantly. Minimum, maximum and mean values here are 0, 513 and 121 pieces cm^{-3}, respectively.

Pollen analysis

Pollen taxon diversity varied down the Nyabuiyabui sediment core with >70 pollen types (Supporting Information, Fig. S1; Table 3) observed and enumerated. The sample with the highest diversity had 68 pollen taxa identified while the sample with the lowest had 18 pollen taxa identified. To aid interpretation and discussion, only the most common pollen types or those types that consistently contributed >2% to the pollen sum for any level are presented, although the full spectra were used for cluster analysis and were grouped into Afromontane, trees, shrubs, herbs and aquatic taxa (Fig. 5; Table 3). Aquatic taxa included *Ludwigia*, Nymphaeae,

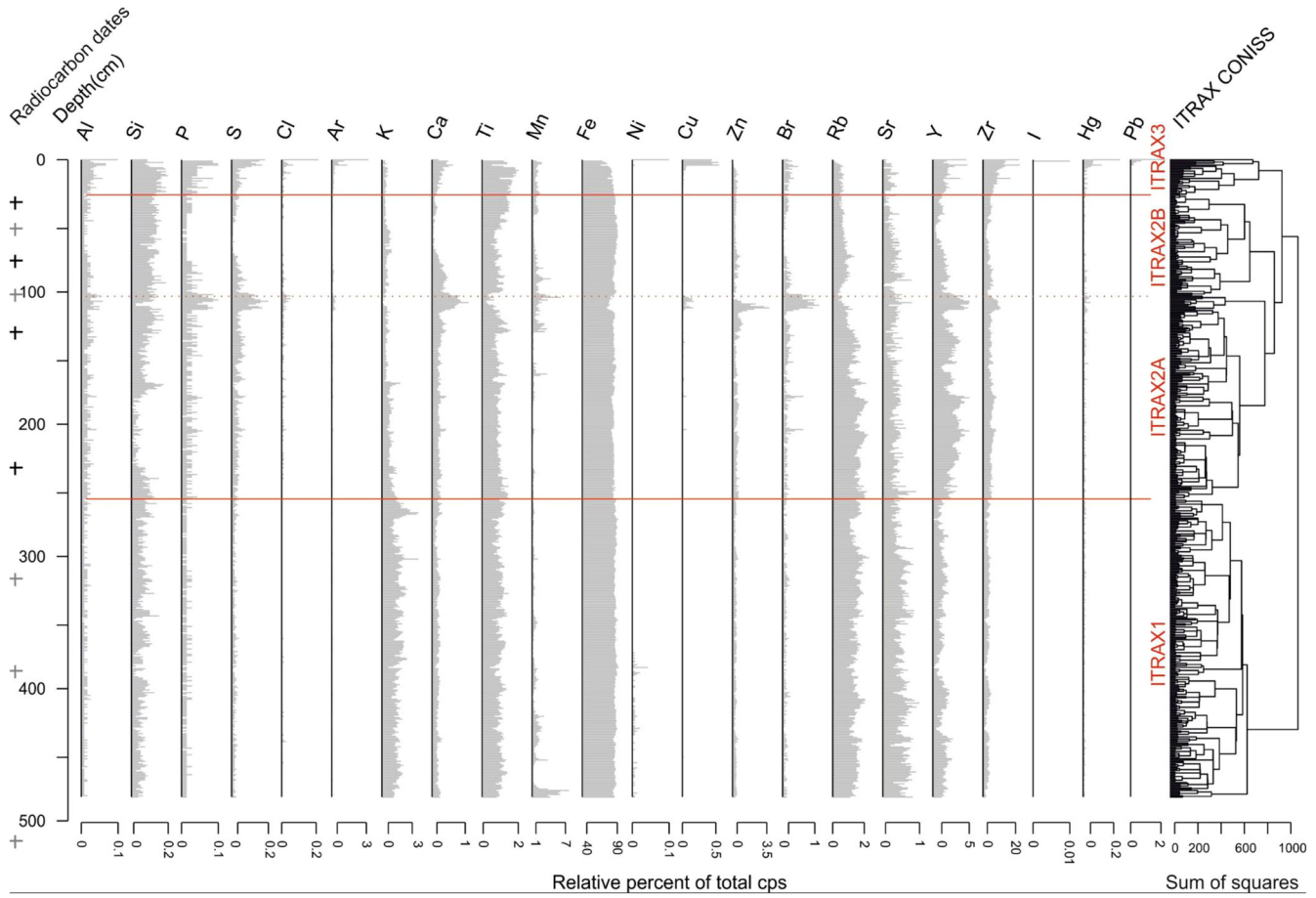

Figure 4. A stratigraphic plot of the sediment elemental characterization using ITRAX (expressed as relative abundance of cps, counts per second) alongside the CONISS dendrogram (Bennett, 1996) which divided the record into three significant zones. The element iodine (I) was also measured, but did not have values above the analytical detection limit of the ITRAX scanner. Radiocarbon dates, '+' symbols on the left. [Color figure can be viewed at wileyonlinelibrary.com]

Cyperaceae and *Typha*. *Cupressus* and *Pinus* are Neophytes that appear in the record during the last ~200 years. Table 3 contains the list of taxa that comprise each grouping.

Throughout the sediment core, Afromontane pollen accounted for ~24% of the taxa (ranging from 12 to 44%), ree pollen accounted for ~15% (0 to 27%), shrub pollen accounted for 8% (0 to 15%), herb pollen accounted for 34% (21 to 37%), aquatics accounted for ~13% (2 to 35%), Poaceae accounted for 7% (0 to 18%) while unknown pollen accounted for ~0.4% (0 to 1%) (Fig. 5).

The pollen diagram was divided into three significant pollen zones using a broken-stick and clustered hierarchical analysis (Bennett, 1996) (Fig. 5). The lowermost pollen zone NBPOLL1 extended from the bottom of the core to 340 cm (the end of the Pleistocene). Afromontane taxa accounted for ~28%, with *Podocarpus*, *Cordia* and *Dracaena* dominating at ~3% each. Tree pollen accounted for ~20%, shrubs for ~11%, herbs for ~32% and unknown pollen for ~0.4% (Supporting Information, Fig. S1). In this zone, arboreal pollen (Afromontane, trees and shrubs) accountyed for ~59% and non-arboreal taxa for ~41% (Fig. 5).

The second pollen zone, NBPOLL2, extended from 330 to 100 cm (end of the Pleistocene to the mid-Holocene) and was divided into sub-zone NBPOLL2A from 330 to 220 cm (end of the Pleistocene and Younger Dryas) and sub-zone NBPOLL2B from 210 to 100 cm (Early and Middle Holocene). There was a sharp decrease in the NBPOLL2A pollen counts across all the vegetation types (average sample count of ~970 in zone NBPOLL1 fell to ~390 in zone NBPOLL2A). The Afromontane taxa remained at ~29%, with *Olea*, *Podocarpus* and *Juniperus* each dominating at ~6%. However, the tree and shrub taxa decreased significantly dropped from 20 to 7% and from 11 to 5%, respectively. This was accompanied by an increase in herbs and aquatic taxa from 32 to 34%.

In zone NBPOLL2B, the average for Afromontane taxa fell significantly to ~18% from 29% in the previous zone (Fig. 5). Afromontane genera dominating this zone were *Cordia* (~4%), *Podocarpus* (~4%), *Croton* (~2%) and *Olea* (~2%). Most of the tree, shrub and herbaceous taxa that had disappeared in NBPOLL2A reappear (*Alangium*, *Commiphora*, *Lannea*, *Maytenus*, *Polyscias*, *Syzygium*, *Abutilon*, *Fagonia* and *Rumex*). Tree taxa increased from 7 to 13% while shrub taxa increased

Table 2. List of elements scanned via the ITRAX core scanner

Aluminium – Al	Silica – Si	Phosphorus – P	Sulphur – S	Copper – Cu	Yttrium – Y
Chlorine – Cl	Argon – Ar	Potassium – K	Calcium – Ca	Zinc – Zn	Strontium – Sr
Titanium – Ti	Manganese – Mn	Iron – Fe	Rubidium – Rb	Bromine – Br	Lead – Pb
Zirconium – Zr	Iodine – I	Mercury – Hg	Nickel – Ni		

Table 3. Pollen taxa identified from the analysis of the 537-cm core collected from Nyabuiyabui

Afromontane	Trees	Shrubs	Herbs	Aquatics
Apodytes	*Allophylus*	Rubiaceae	Laportea	*Ludwigia*
Celtis	*Annona*	*Salvadora*	Malvaceae	Nymphaceae
Cordia	*Carissa*	*Schefflera*	*Ormocarpum*	Cyperaceae
Croton	Combretaceae	*Syzygium*	*Phyllanthus*	*Typha*
Cupressus *	*Commiphora*	*Tarchonanthus*	*Plantago*	
Dracaena	*Lannea*	*Abutilon*	*Rumex*	
Ficus	*Maerua*	Acanthaceae	*Sansevieria*	
Hagenia	*Maesa*	*Achyranthes*	Solanaceae	
Juniperus	*Maytenus*	Amaranthaceae/Chenopodiaceae	Umbelliferae	
Olea	*Monotes*	Asteraceae	*Urtica*	
Podocarpus	*Morella (Myrica)*	*Blaeria*	*Vernonia*	
Prunus	*Myrsine*	Brassicaceae	Capparidaceae	
Alangium	*Pinus* *	*Cadaba*	*Cissus*	
	Polyscias	Fabaceae	*Commelina*	
	Psidium	*Cyathula*	*Fagonia*	
	Rhus	*Erica*	*Gomphrena*	
		Euphorbia	*Heliotropium*	
		Hypericum	*Hypoestes*	
		Impatiens	Liliaceae	
		Ipomoea	*Narcissus*	
		Justicia	*Polygonum*	
			Ruellia	
			Trianthema	
			Poaceae	

* *Pinus* and **Cupressus* are agroforestry neophytes at the study site.

from ~5 to ~7%. Herbaceous and aquatic taxa increased to 40 and 11%, respectively.

The third pollen zone (NBPOLL3) extends from 90 cm to the top (Late Holocene to present), where the average Afromontane pollen taxa reduced to 16%, tree pollen remained at ~12%, and shrubs remained ~7%. Herbs fell significantly to ~24% from 40% while the aquatic taxa and Poaceae increased to ~24 and ~13%, respectively. The aquatics and Poaceae in this zone were at their highest recorded level. *Podocarpus* (~5%), *Cordia* (~3%), *Ficus* (~3%), *Commiphora* (~2%) and *Rhus* (~2%) dominate this zone. Introduced tree taxa (Neophytes), namely *Cupressus* and *Pinus*, appear towards the top of the sediment core (20 cm) at high abundance as they were introduced taxa at commercial timbering scales and frequently used on residential and industrial properties.

Pollen taxa, charcoal concentration, organic matter content, clay, sand and some elements/elemental ratios are plotted alongside the lithology and radiocarbon dates. Summary aspects

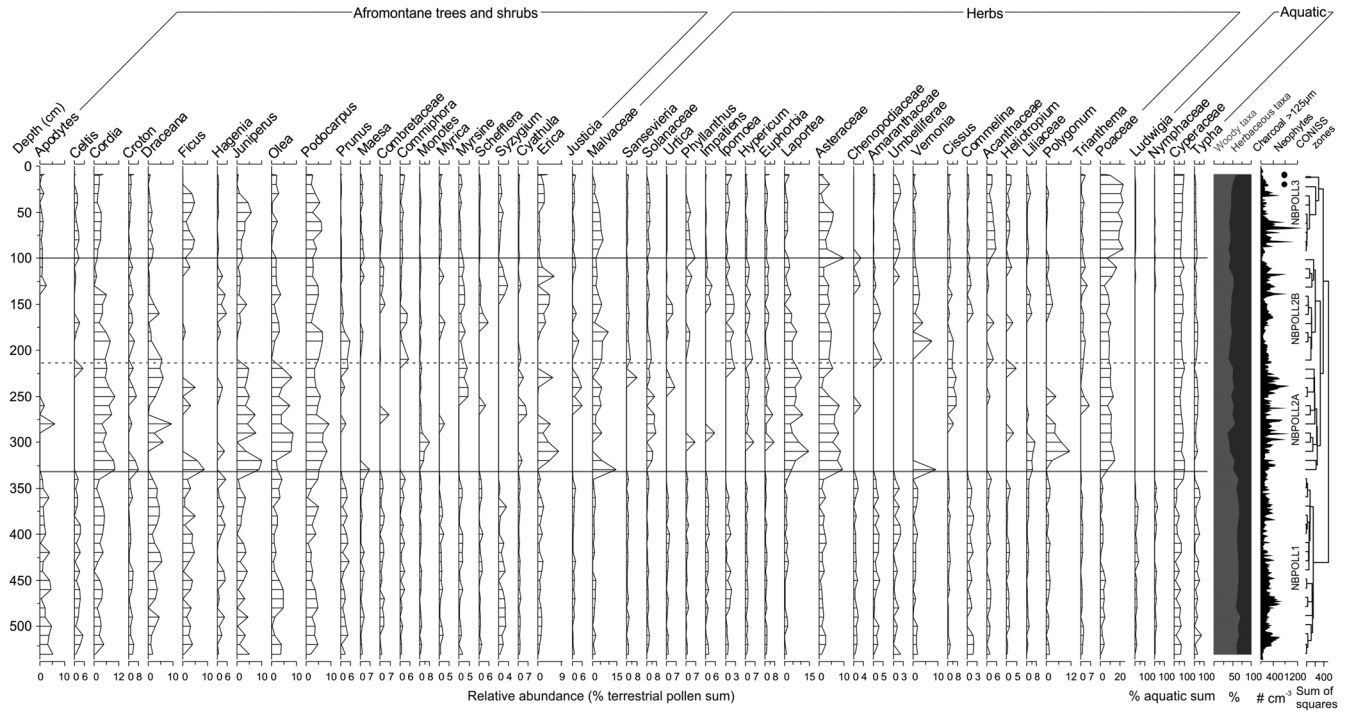

Figure 5. Relative pollen abundances of the terrestrial pollen sum from the Nyabuiyabui sediment core, radiocarbon dates ('+' symbols on the left, black font for dates used in the suggested age–depth model in Fig. 2) and charcoal (>125 µm) for comparison. Aquatic taxa are shown as relative abundances of the total aquatic pollen sum (Table 2).

from the different proxies are plotted in a single stratigraphic plot (Fig. 6) to ease comparison across datasets. Significant changes in each of the proxies occurs at around the same time, implying that the changes noted have the same or similar drivers.

Discussion

The Nyabuiyabui wetland sediment record covers the interval from the end of the Late Pleistocene (~17 000 cal a BP) to the present and provides insight into the dynamics of the wetland as well as the wider Mau Forest ecosystem. Given its geographical location, insights from the Nyabuiyabui sediment record have relevance for areas downstream within the Sondu and the Mara River catchment. The results also provide another comparison point of long-term environmental change in the East African highlands.

Although lacustrine sedimentary archives are often preferred due to their high time resolution and reliable dating (Ojala *et al.*, 2012), the lack of undisturbed lakes in the Mau Forest necessitates investigations of wetland palustrine sediments to generate knowledge of past ecosystem and environmental changes. The temporal resolution of wetland sediment records in eastern Africa is variable and these shallow-water ecosystems frequently experience higher levels of physical and bioturbation due to their small size and volume compared to lakes (Rucina *et al.*, 2010; Githumbi, 2017). Sedimentary hiatuses have frequently been observed during the Late Pleistocene to Early Holocene from lacustrine and palustrine sediment records across eastern Africa, such as the Rukiga Highlands (Taylor, 1990), Laikipia Plateau (Taylor *et al.*, 2005), Munsa in Uganda (Lejju *et al.*, 2005), Mount Kenya (Street-Perrott *et al.*, 2007; Rucina *et al.*, 2009), Eastern Arc Mountains in Tanzania (Mumbi *et al.*, 2008; Finch *et al.*, 2009, 2014), Pare Mountains in Tanzania (Heckmann, 2014), the Rufiji Delta (Punwong *et al.*, 2013) and Virunga (McGlynn *et al.*, 2013).

The distribution of radiocarbon dates collected from Nyabuiyabui is complex and reveals some age–depth reversals, which has been observed in several palustrine sediment studies in the region (Hamilton, 1982; Courtney Mustaphi and Marchant, 2016). This has been observed in lowland wetlands (Awuor, 2008; Öberg *et al.*, 2012; Githumbi *et al.*, 2018a,b; Goman *et al.*, 2020) and montane wetlands (Bonnefille and Riollet, 1988; Mumbi *et al.*, 2008; Finch *et al.*, 2009). The radiocarbon dates from Nyabuiyabui group the sediment stratigraphy into a basal pre-Holocene (Late Pleistocene), Early to Mid-Holocene, and Late Holocene section. By focusing our age–depth model on the dates that are derived from macrofossils, we are able to construct a coherent age–depth relationship that is very useful for assessing broad patterns of sedimentological and vegetation change at Nyabuiyabui (Fig. 6). Similar to several other palaeoenvironmental records established from palustrine sediments, the radiocarbon date uncertainties limit the precision of exploring the specific timing of events or rates of change. However, the vegetation change is explored and discussed with reference to depth to acknowledge this uncertainty. We describe the long-term variability in forest composition and fire during the broad periods of the Late Pleistocene, Early to Mid Holocene and Late Holocene.

Changes in pollen composition and abundance throughout the core indicate the persistence of an upland forest dominated by *Podocarpus*, *Cordia*, *Juniperus* and *Olea* with varying degrees of openness possibly caused by ecological turnover and a variable fire regime. *Podocarpus*, *Cordia*, *Juniperus* and *Olea* appear in all the samples, Afromontane taxa in general appear in all pollen zones. Pollen zone NBPOLL2A (Late Pleistocene to Early Holocene transition period) experienced a loss of montane forest taxa (*Abutilon*, *Alangium*, *Commiphora*, *Fagonia*, *Lannea*, *Maytenus*, *Polyscias*, *Psidium*, *Rumex* and *Syzygium*). The disappearance as well as the general decrease in tree and shrub taxa is accompanied by an increase in Poaceae and aquatic taxa. This suggests a drying environment with a contraction in the open water area providing more extensive shallow-water littoral areas for taxa such as *Typha* and Cyperaceae to become established. The general trend towards the top of the core is an increase in herbaceous taxa compared to the woody taxa.

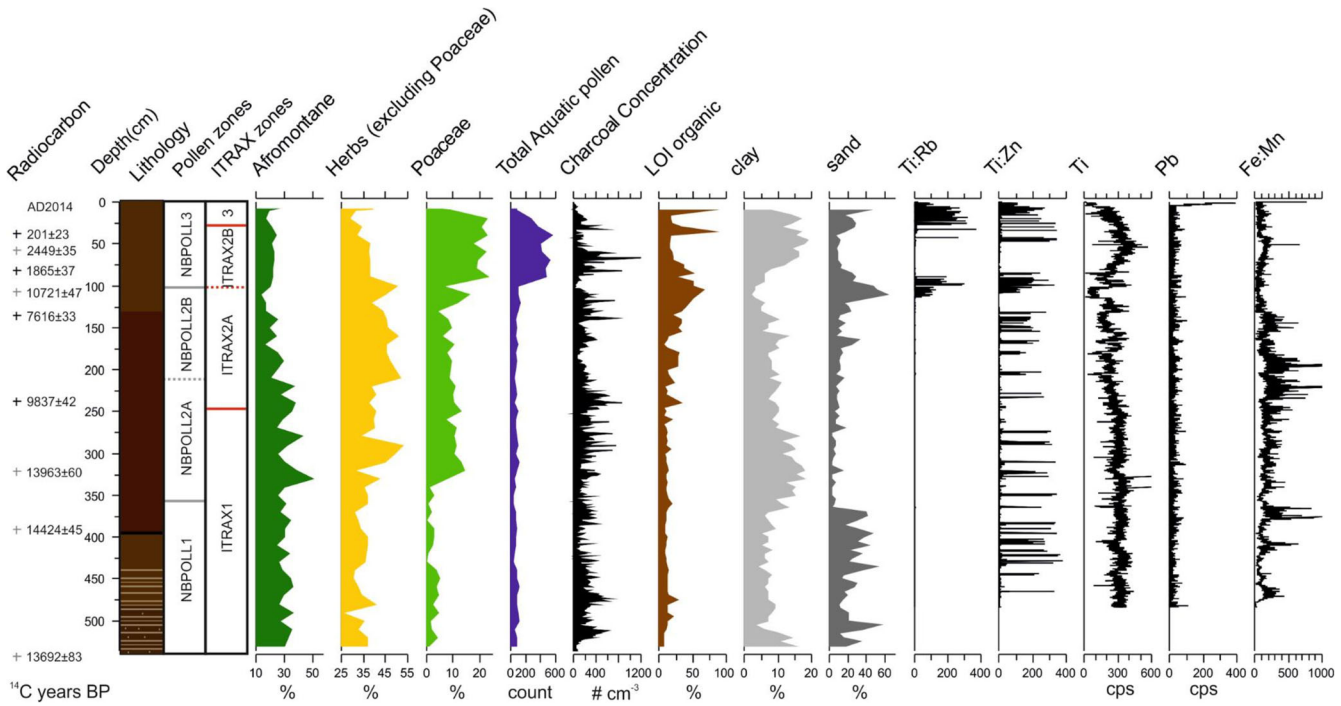

Figure 6. A stratigraphic plot of radiocarbon dates, lithology and pollen and ITRAX CONISS zonations, and select palaeoecological and sedimentological measurements. Pollen percentages are grouped into Afromontane and herbs, Poaceae, and aquatic pollen counts, as well as charcoal (>125 μm), organic, clay and sand contents. [Color figure can be viewed at wileyonlinelibrary.com]

Late Pleistocene to Early Holocene development of Eastern Mau: 538–240 cm

The end of the Late Pleistocene (540–220 cm) exhibits the highest arboreal pollen diversity (number of taxa identified) and abundance (total counts in each sample) while the herbs and grasses are at minimal abundances. This diversity is in part due to turnover at 330 cm to an ecosystem dominated by *Cordia, Croton, Ficus, Juniperus* and *Olea* from one dominated by *Apodytes, Celtis, Dracaena, Hagenia* and *Podocarpus*. The turnover signifies a change from Afromontane taxa that prefer a cooler, dry environment to one characterized by more mesic conditions. This ecosystem transition is similar to that documented by pollen records from the Rukiga Highlands (Taylor, 1990), Ruwenzori (Livingstone, 1967), Burundi highlands (Bonnefille and Riollet, 1988), Lake Albert (Beuning *et al.*, 1997), Mount Elgon (Hamilton, 1987) and Mount Kenya (Street-Perrott *et al.*, 2007; Rucina *et al.*, 2009). This interval is also characterized by the highest biomass burning with high macroscopic charcoal concentrations implying a continuous connected source of fuel. *Juniperus*, a pioneer species colonizing gaps after a fire, is a dominant taxon in this forest transition, and more broadleaved species such as *Olea* are also established. The successional role of *Juniperus* in forests with recurring fire events is observed on Mount Kenya (Rucina *et al.*, 2009) and the southern Aberdare Range (Bussmann, 2001). In the Nyabuiyabui pollen record, peaks in *Juniperus* lag behind those in *Hagenia* and may signal a sequence of ecological response to fire. The increase in Afromontane and tree taxa corresponds to increases in magnetic susceptibility, silt and clay as well as peaks in detrital elements. The detrital elements, silicon (Si), titanium (Ti), iron (Fe), rubidium (Rb) and strontium (Sr), show increased terrigenous input indicating higher erosional inputs to the basin through surface runoff conditions after episodes of heavy or continuous rainfall.

Several East African Pleistocene palaeoenvironmental records are dominated by signals inferring cooler, dryer conditions such as forest compositional changes to semi-deciduous forest and lower lake levels (Van Zinderen Bakker and Coetzee, 1988; Sonzogni *et al.*, 1998; Olago, 2001; Chalié and Gasse, 2002). Late Pleistocene sediments from the Rumuiku Swamp from Mount Kenya or the Lake Emakaat record show stratigraphic changes as well as increases in wetland fringe taxa (Cyperaceae, Poaceae and *Typha*), indicating lower water levels (Ryner *et al.*, 2006; Rucina *et al.*, 2009). However, the Lake Challa record indicates increased precipitation due to the intensification of the south-easterly Indian Ocean Monsoon from ~16 500 cal a BP to the Early Holocene that was interrupted during the Younger Dryas between ~13 300 and 11 700 cal a BP (Verschuren *et al.*, 2009).

The varied responses among palaeo-vegetation data from different highland areas of equatorial eastern Africa suggest heterogeneity in hydroclimate–vegetation interactions since the Late Pleistocene to present day. This is not surprising given the local topographic–climate system feedback or position of the mountain in bioclimatic space being important controls on the response of the ecosystem through time (Hamilton, 1982; Loomis *et al.*, 2017; Los *et al.*, 2019). The drivers responsible for changes through time recorded by multiple palaeoenvironmental proxies across different mountains are uncertain; even for those records that are characterized by similar climate change, there are localized factors such as topography, hydrology and soil development to take into account. Given the differential response across the East African Mountains, a comparison of available studies across mountain ranges will improve our understanding of coherent responses across different mountain ecosystems and lead to an understanding of typologies of ecosystem response to rapid climate transitions.

The Early and Middle Holocene: 240–100 cm

At Nyabuiyabui, the low Ti, Fe and Mn concentrations in the sediments from 256 to 213 cm could indicate increasing dryness (Burrows *et al.*, 2016). There is also a marked decrease in the number of pollen taxa identified and abundance until 190 cm, while the contribution of Poaceae pollen increases, implying a relatively warm and dry interval. The forest becomes increasingly open after 190 cm (the Early Holocene), and the subalpine forest association of *Hagenia–Juniperus* is interpreted as an early succession phase following fire-induced disturbance (Bussmann, 2001). There is an increase in *Apodytes, Celtis, Olea, Podocarpus* and *Erica* representative of montane forest. On Kilimanjaro, a warm and wet climate enabled the development and expansion of Afromontane forest around this period (Schüler *et al.*, 2014). The Early Holocene experienced the highest increase in organic matter and decrease in carbonate content, accompanied by an increased silt and clay content as well as increased bulk density, implying high sedimentation. The increased organic matter content peaking with sulphur content could indicate that the increased sedimentation was anoxic (Tierney and Russell, 2007).

Compared to the Late Pleistocene, the climate of equatorial eastern Africa was generally warm and wet (Bonnefille and Riollet, 1988) until ~4000 cal a BP when it became drier and there was more open grassland (Olago, 2001; Msaky *et al.*, 2005; Garcin *et al.*, 2012). Many eastern African lacustrine and palustrine sediment records are characterized by sedimentary hiatuses around the Early Holocene, reducing the number of available study sites that contribute to our understanding of vegetation changes occurring in those temporal gaps. The hiatuses cover the African Humid Period in which several eastern African lakes reached their highest levels (Hoelzmann *et al.*, 2004; Foerster *et al.*, 2015; Dallmeyer *et al.*, 2019). Most of these lakes overflowed and merged with other lakes or rivers; for example, Lake Turkana temporarily overflowed into the White Nile (Garcin *et al.*, 2012), Lake Kivu overflowed and the Ruzizi River overflowed into Lake Tanganyika (Haberyan and Hecky, 1987). At Nyabuiyabuyi, organic matter gradually decreases, indicating an autochthonous source of sediment in the wetland (Burrows *et al.*, 2016). The detrital elements (Si, Ti, Fe, Rb and Sr) decrease and reach a plateau with increased amount of organic matter content. The decline in elemental counts may reflect the ecosystem becoming more drought-adapted; lower precipitation leading to reduced sedimentation through runoff would account for the very low counts of Ti, Fe and Mn and elevated Br levels (Burrows *et al.*, 2016). An increase in Ti, Fe and Zn reflects a much wetter interval than previously; these elements peak and reduce drastically, implying a wet interval that ends abruptly. The dark brown sediment from 350 cm to the top has no laminations; this could indicate sediment reworking, resuspension or benthic fauna mixing up the sediments as observed in the Lake Tanganyika sediment (Haberyan and Hecky, 1987). The charcoal record for the Younger Dryas/Early Holocene shows slightly lower concentraions than during the Late Pleistocene, but this increased significantly during the Middle Holocene to reach the highest charcoal concentrations.

The Late Holocene: 100 cm to the top

Increasingly arid conditions are recorded in the Nyabuiyabui record with continued replacement of Afromontane taxa with

arboreal taxa that tolerate drier conditions (*Cordia*, *Hagenia* and *Podocarpus*). Locally there is an increase in aquatic taxa (Cyperaceae/*Typha*), which could reflect the expansion of wetland margins. Poaceae and the highest NPP counts (non-pollen palynomorph data not presented) suggest an intensification in the use of the wetland by herbivores. This would occur during an arid interval due to necessity and increased access due to lower water levels (Gelorini *et al.*, 2012) or possibly as result of greater use of the area for agro-pastoralism.

The highland ecosystems of eastern Africa, such as Mount Kenya, experienced pronounced ecosystem shifts through the Late Holocene (Street-Perrott *et al.*, 2007; Rucina *et al.*, 2009) due to varying arid and mesic environmental conditions as recorded by dramatic ecosystem and lake level changes (Marchant *et al.*, 2018). Some of these transitions were relatively slow while others were more dramatic with a wide spatial signature. For example, continent-wide aridity (Marchant and Hooghiemstra, 2004) is noted around 4000 cal a BP after which eastern African lake levels fluctuate markedly in responce to intervals of varying rainfall and aridity (Gasse, 2000; Verschuren *et al.*, 2000; Cohen *et al.*, 2005; Garcin *et al.*, 2012). Lake Rukwa becomes and remains saline within most of the last 5000 cal a BP with several probable dry periods marked by hiatuses in the core (Barker *et al.*, 2002).

Global transformations of the landscape are hypothesized to have reached significant levels globally ~3000 cal a BP (Ellis *et al.*, 2013). Data from eastern Africa indicate a shift in the adoption of livelihood patterns, for example as indicated by Wright (2005) while exploring resource exploitation among Neolithic hunters and herders. The spread of agropastoralism in Africa is believed to have occurred from 4000 cal a BP, altering landscapes through grazing and cultivation (Archibald *et al.*, 2012; Phelps *et al.*, 2020). Different land-use activities began in Kenya ~4000 cal a BP, i.e. pastoralism at ~4000 cal a BP, extensive agriculture at ~1000 cal a BP and intensive agriculture ~500 cal a BP, and foraging declines ~250 cal a BP (Stephens *et al.*, 2019). Archaeological studies in this landscape would improve our understanding of resource use in the catchment; unfortunately, the two closest archaeological sites (burial caves) have not unearthed information about forest and wetland resource use (Faugust and Sutton, 1966; Merrick and Monaghan, 1984).

Several severe arid events are recorded during the Late Holocene; a diatom–chironomid record from Lake Naivasha using salinity to infer lake levels over the last 1100 years shows several intervals more arid than any recorded in the 20th century (Verschuren *et al.*, 2000). Sediments from Lake Tanganyika and Lake Kivu record salinity peaks with Lake Kivu having salinity levels three times higher than the modern lake (Haberyan and Hecky, 1987). Within the Nyabuiyabui record, geochemical analysis shows a drop in all element concentrations except Cl, Ar, Cu, Hg and Pb. Increased Cl often results from precipitated chloride of NaCl that occurs during dry conditions (Kristen, 2009). The Ti/Rb ratio is useful to understand sediment source (Arnaud *et al.*, 2014): this peaks twice in the Late Holocene (Fig. 6) at the same time as the Ti/Zn ratio and increases in sand and could indicate sedimentation of eroded material in the area. Lake Bogoria records a decline in high-altitude forest taxa (Kiage and Liu, 2006), whereas there is an increase in drought-tolerant taxa on Mounts Kenya and Elgon (Hamilton, 1982; Vincens, 1986), which imply the establishment of more arid conditions. This loss in high-altitude taxa could also be a signal of widespread clearance recorded in several montane forest sites (Bessems *et al.*, 2008; Kiage and Liu, 2009; Rucina *et al.*, 2009; Gelorini *et al.*, 2012) attributed to land use activities across eastern and central Africa.

Significant changes to forest compositions have been inferred from the Eastern Arc Mountains during the past 2000 cal a BP (Heckmann, 2014; Finch *et al.*, 2017) that potentially relate to intensified mountain forest resource use (Iles *et al.*, 2018). A sediment record from the Mara basin records a significant increase in sedimentation as well as increasing Hg levels from the late 1700s (Dutton *et al.*, 2019) that resonates with our insights from the sedimentary record. In the Nyabuiyabui record, there are high levels of introduced *Cupressus* and *Pinus* taxa, and increased levels of Asteraceae, Acanthaceae and *Vernonia*. *Cupressus* and *Pinus* provide markers for the onset of colonial forestry operations in the early part of the 20th century (Finch *et al.*, 2014). There is an increasing trend in element concentrations, with spikes in Cu, S, Hg, Ar and Pb towards the top of the sediment record (~25 cm). The onset of the increase corresponds to the advent of industrialization and thus in deposition of heavy elements while the later changes would be due to increased human presence and mechanized agroforestry (Troup, 1932). The Upper Mara was identified as a major source of sediment in the Mara wetland (Dutton *et al.*, 2019) and so increased sedimentation would correspond to increased erosion and runoff in the upper Mara. In recent history (~200 years), eastern African montane forests were either reserved, industrially logged or maintained locally as culturally valued spaces during colonial government rule. Many Afromontane forests were converted to agroforests by the 1930s (Troup, 1932; Wood, 1965) with the Kenya Forest Service managing the higher elevation forests for timber production in public–private partnerships following independence.

Recent land-cover change within the Mau Forest (Landsat data from 1986) indicates that forest cover has consistently shrunk in areal extent with an increase in cropland and grassland cover. These changes are correlated strongly with rapid population increase (Odawa and Seo, 2019). Increased population pressure leading to deforestation and illegal logging, together with land cover conversion, mainly to agriculture and settlement, in the Mau escarpment have been identified as contributing to the overall degradation of the Mara basin and changed hydrological and sedimentation regime (Defersha and Melesse, 2012). The upper catchment of the Mara River drains south-east of Mau, with 65% of the catchment area located in Kenya and the rest in Tanzania (Defersha and Melesse, 2012; Mwangi *et al.*, 2016a) covering both the Maasai-Mara and Serengeti wildlife areas and important wetland areas in estuaries with Lake Victoria, such as Lake Masirori (Dutton *et al.*, 2019).

The two main Mau land cover types are forest and grassland, in which rapid conversion to cropland and bare land is taking place. Controlling for slope, organic matter content and extreme rainfall events, a study combining field and modelling data to understand the effects of the land-cover change in the Mara basin identified deforestation as a significant cause of change in water quality and watershed degradation, particularly in the upper sections of the Amala and Nyangores tributaries into the Mara River (Defersha and Melesse, 2012). A study by Mwangi *et al.* (2016b), using the Soil and Water Assessment Tool (SWAT) to understand the effects of agroforestry on the Mara hydrology, concluded that agroforestry impacts cannot be generalized across a catchment without considering climate variability within the watershed. Increased deforestation and conversion to agriculture in the Mau Highlands increases the variability of catchment water flows. As observed in a paired study in the Kapchorwa catchment, peak discharge flow increased significantly after the deforestation of the Nanadi/Kakamega tropical rainforest due to the loss of ground cover that regulates surface runoff (Mwangi *et al.*, 2016a,b). However, areas under current

agricultural production when converted to agroforestry lead to a decrease in runoff while increasing groundwater uptake – this is often because of the choice of tree species sich as *Eucalyptus* that has a massive water demand (Hubbard *et al.*, 2020). Land use, predominantly deforestation and transition to agriculture, was found to influence nitrous oxide levels in the lower elevations of the Mara River network (Mwanake *et al.*, 2019). The effect of forest cover loss leading to reduced capacity to act as a catchment during heavy rainfall and mediate streamflow was identified as a major disruptor to economic activities to the south-west of Mau (Otuoma *et al.*, 2012). Various streams connecting into the Sondu River catchment experience steep increases (floods) after a heavy downpour followed by long intervals of very low stream flow. This has adverse effects on tea plantations and the Sondu hydroelectric power station, which cannot adequately predict waterflow needed for planning (Otuoma *et al.*, 2012).

Despite the net loss in forest cover, some cropland and grassland areas have converted back to forest (Odawa and Seo, 2019). Natural regeneration coupled with reforestation and conservation efforts can be applied to curb and even reverse the impacts of forest loss (Marshall *et al.*, 2020). Thus, the Mau forest management efforts need to consider the impacts of forest activities not only on the forest ecosystem, the interactions of local populations with this, and wider hydrological issues across the basins at national and regional levels.

Conclusions

Nyabuiyabui is a unique montane forest wetland record providing insights into long-term forest dynamics due primarily to climate change as well as long-term wetland development for the largest last remaining closed-canopy forest in eastern Africa, with significant impacts across the wider landscape including the Mara river system. The Nyabuiyabui catchment has undergone significant changes in forest composition from a highly diverse Afromontane to a more open forest ecosystem indicative of increased aridity in the region.

Precipitation change is an important driver of vegetation composition over time. The additional effects of fires have been an important component of Mau forests, glades and vegetated wetlands. At Nyabuiyabuyi, the significant increase in elements such as Pb and Hg over the last 200 cal a BP combined with the rise of exotic taxa are clear indicators of human forestry activity at industrial scale that would impact forest ecosystems and associated service delivery across the catchment. Further focused studies on other wetlands located along the Mau Forest complex would greatly improve our understanding of the recent past and interpret how these changes on forest cover impact on hydrology and downstream impacts.

Managing and ensuring an intact and functioning forest-hydrological system is vital for the Mau Highlands and the wider lowland savanna ecosystems and livelihoods. Long-term data on vegetation change of highland watersheds provide useful context for current climate and land use change debates and how these insights can support management decisions for remediation efforts and future restoration outcomes.

Supporting information

Additional supporting information may be found in the online version of this article at the publisher's web-site.

Figure S1. A stratigraphic plot of the complete pollen taxa identified and the associated CONISS pollen assemblage zonation.

Acknowledgements. We thank Rebecca Muthoni, Nicholas Gakuu, Joseph Mutua, the National Museums of Kenya and the British Institute in Eastern Africa for research support; and Professor Henry Lamb for his invaluable advice on ITRAX core scanning. The National Commission for Science, Technology and Innovation issued permits for this research (NACOSTI/P/14/6965/1096). E.N.G. and C.C.M. were supported through the 'Resilience in East African Landscapes' (REAL) project funded by a European Commission Marie Skłodowska-Curie Actions Initial Training Network grant to R.M. and Paul Lane as PI (FP7-PEOPLE-2013-ITN project No. 606879). C.C.M. was also supported through the 'Adaptation to Climate Change' (ARCC) project funded by the Sustainability and Resilience – tackling climate and environmental changes programme of the Swedish Research Council (Vetenskapsrådet), Sida and Formas (2016-06355) awarded to Paul Lane and R.M. and led through Uppsala University. C.C.M. benefited through the World Bank Africa Centers of Excellence (ACEII) programme exchange visits with WISE-FUTURES, Nelson Mandela African Institution of Science and Technology, Arusha. This study formed part of the PhD dissertation of E.N.G., University of York, and is a contribution to the Past Global Changes (PAGES) supported Global Paleofire (GPWG2) and LandCover6k Working Groups. PAGES is funded by the Swiss Academy of Sciences and Chinese Academy of Sciences and supported in-kind by the University of Bern.

Abbreviations. asl, above sea level; LOI, loss-on-ignition; XRF, X-ray fluorescence.

References

Archibald S, Staver AC, Levin SA. 2012. Evolution of human-driven fire regimes in Africa. *Proceedings of the National Academy of Sciences of the United States of America* **109**: 847–852.

Arnaud F, Atahan P, Ausili A *et al.* 2014. Micro-XRF studies of sediment cores. Smol, John P., Croudace, Ian W. & Rothwell, Guy R., *Developments in Paleoenvironmental Research*. Springer, Applications of a non-destructive tool for the environmental sciences. **17**: Ontario.–668. https://link.springer.com/book/10.1007%2F978-94-017-9849-5

Awuor OJ. 2008. *Palaeoclimate of Ondiri swamp*. Master's Thesis, University of Nairobi

Bamber RN. 1982. Sodium hexametaphosphate as an aid in benthic sample sorting. *Marine Environmental Research* **7**: 251–255.

Barker P, Telford R, Gasse F *et al.* 2002. Late Pleistocene and Holocene palaeohydrology of Lake Rukwa, Tanzania, inferred from diatom analysis. *Palaeogeography, Palaeoclimatology, Palaeoecology* **187**: 295–305.

Barker PA, Street-Perrott FA, Leng MJ *et al.* 2001. A 14,000-year oxygen isotope record from diatom silica in two alpine lakes on Mt. Kenya. *Science* **292**: 2307–2310.

Bennett KD. 1996. Determination of the number of zones in a biostratigraphical sequence. *New Phytologist* **132**: 155–170.

Bessems I, Verschuren D, Russell JM *et al.* 2008. Palaeolimnological evidence for widespread late 18th century drought across equatorial East Africa. *Palaeogeography, Palaeoclimatology, Palaeoecology* **259**: 107–120.

Beuning KRM, Talbot MR, Kelts K. 1997. A revised 30,000-year paleoclimatic and paleohydrologic history of Lake Albert, East Africa. *Palaeogeography, Palaeoclimatology, Palaeoecology* **136**: 259–279.

Blaauw M. 2010. Methods and code for 'classical' age-modelling of radiocarbon sequences. *Quaternary Geochronology* **5**: 512–518.

Blaauw M, Christen JA. 2011. Flexible paleoclimate age–depth models using an autoregressive gamma process. *Bayesian Analysis* **6**: 457–474.

Blaauw M, Christen JA, Bennett KD *et al.* 2018. Double the dates and go for Bayes – impacts of model choice, dating density and quality on chronologies. *Quaternary Science Reviews* **188**: 58–66.

Bonnefille R, Riollet G. 1988. The Kashiru Pollen Sequence (Burundi) Palaeoclimatic Implications for the last 40,000 yr B.P. in Tropical Africa. *Quaternary Research* **30**: 19–35.

Bonny AP. 1972. A method for determining absolute pollen frequencies in lake sediments. *New Phytologist* **71**: 393–405.

Burrows MA, Heijnis H, Gadd P *et al.* 2016. A new late Quaternary palaeohydrological record from the humid tropics of northeastern

Australia. *Palaeogeography, Palaeoclimatology, Palaeoecology* **451**: 164–182.
Bussmann RW. 2001. Succession and regeneration patterns of East African mountain forests. A review. *Systematics and Geography of Plants* **71**: 959.
Chalié F, Gasse F. 2002. Late Glacial–Holocene diatom record of water chemistry and lake level change from the tropical East African Rift Lake Abiyata (Ethiopia). *Palaeogeography, Palaeoclimatology, Palaeoecology* **187**: 259–283.
Chapman LJ, Balirwa J, Bugenyi FWB *et al*. 2001. Wetlands of East Africa: biodiversity, exploitation, and policy perspectives. *Biodiversity in Wetland: Assessment, Function and Conservation* **2**.
Cohen AS, Palacios-Fest MR, Msaky ES *et al*. 2005. Paleolimnological investigations of anthropogenic environmental change in Lake Tanganyika: IX. Summary of paleorecords of environmental change and catchment deforestation at Lake Tanganyika and impacts on the Lake Tanganyika ecosystem. *Journal of Paleolimnology* **34**: 125–145.
Colombaroli D, van der Plas G, Rucina S *et al*. 2018. Determinants of savanna-fire dynamics in the eastern Lake Victoria catchment (western Kenya) during the last 1200 years. *Quaternary International* **488**: 67–80.
Courtney Mustaphi C, Marchant R. 2016. A database of radiocarbon dates for palaeoenvironmental research in Eastern. *Africa. Open Quaternary* **2**: 1–7.
Courtney Mustaphi CJ, Githumbi EN, Shotter LR *et al*. 2016. Subfossil statoblasts of *Lophopodella capensis* (Sollas, 1908) (Bryozoa, Phylactolaemata, Lophopodidae) in the Upper Pleistocene and Holocene sediments of a montane wetland, Eastern Mau Forest, Kenya. *African Invertebrates* **57**: 39–52.
Courtney Mustaphi CJ, Kinyanjui R, Shoemaker A *et al*. 2020. A 3000 year record of vegetation changes and fire at a high-elevation wetland on Kilimanjaro, Tanzania. *Quaternary Research*.
Cranworth Betram Francis Gurdon. 1912. *A Colony in the Making: or, Sport and Profit in British East Africa/by Lord Cranworth*. Macmillan: London: 448. https://www.biodiversitylibrary.org/bibliography/27475#/summary
Croudace IW, Rindby A, Rothwell RG. 2006. ITRAX: description and evaluation of a new multi-function X-ray core scanner, *Geological Society, London, Special Publications* (51–63.
Cuní-Sanchez A, Pfeifer M, Marchant R *et al*. 2016. Ethnic and locational differences in ecosystem service values: insights from the communities in forest islands in the desert. *Ecosystem Services* **19**: 42–50.
Dallmeyer A, Claussen M, Lorenz SJ *et al*. 2019. The end of the African humid period as seen by a transient comprehensive Earth system model simulation of the last 8000 years. *Climate of the Past Discussions* 117–140.
De Cort G, Verschuren D, Ryken E *et al*. 2018. Multi-basin depositional framework for moisture-balance reconstruction during the last 1300 years at Lake Bogoria, central Kenya Rift Valley. *Sedimentology* **65**: 1667–1696.
Defersha MB, Melesse AM. 2012. Field-scale investigation of the effect of land use on sediment yield and runoff using runoff plot data and models in the Mara River basin, Kenya. *CATENA* **89**: 54–64.
Demenocal P, Ortiz J, Guilderson T *et al*. 2000. Abrupt onset and termination of the African Humid Period: rapid climate responses to gradual insolation forcing. *Quaternary Science Reviews* **19**: 347–361.
Dutton CL, Subalusky AL, Anisfeld SC *et al*. 2018. The influence of a semi-arid sub-catchment on suspended sediments in the Mara River, Kenya. *PLoS ONE* **13** e0192828.
Dutton CL, Subalusky AL, Hill TD *et al*. 2019. A 2000-year sediment record reveals rapidly changing sedimentation and land use since the 1960s in the Upper Mara-Serengeti Ecosystem. *Science of the Total Environment* **664**: 148–160.
Ellis EC, Kaplan JO, Fuller DQ *et al*. 2013. Used planet: a global history. *Proceedings of the National Academy of Sciences of the United States of America* **110**: 7978–7985.
Erdtman G. 1960. The acetolysis method-a revised description. *Svensk Botanisk Tidskrift* **54**: 516–564.
Faegri K, Iversen J. 1950. *Textbook of Modern Pollen Analysis*. Ejnar Munksgaard: Copenhagen.–167.
Faegri K, Iversen J. 1989. *Textbook of Pollen Analysis IV Edition*. John Wiley & Sons, IV, New York.–328.
Faugust PM, Sutton JEG. 1966. The Egerton cave on the Njoro River. *Azania: Archaeological Research in Africa* **1**: 149–153.
Finch J, Leng MJ, Marchant R. 2009. Late Quaternary vegetation dynamics in a biodiversity hotspot, the Uluguru Mountains of Tanzania. *Quaternary Research* **72**: 111–122.
Finch J, Marchant R. 2011. A palaeoecological investigation into the role of fire and human activity in the development of montane grasslands in East Africa. *Vegetation History and Archaeobotany* **20**: 109–124.
Finch J, Marchant R, Courtney, Mustaphi CJ. 2017. Ecosystem change in the South Pare Mountain bloc, Eastern Arc Mountains of Tanzania. *The Holocene* **27**: 796–810.
Finch J, Wooller M, Marchant R. 2014. Tracing long-term tropical montane ecosystem change in the Eastern Arc Mountains of Tanzania. *Journal of Quaternary Science* **29**: 269–278.
Foerster V, Vogelsang R, Junginger A *et al*. 2015. Environmental change and human occupation of southern Ethiopia and northern Kenya during the last 20,000 years. *Quaternary Science Reviews* **129**: 333–340.
Garcin Y, Melnick D, Strecker MR *et al*. 2012. East African mid-Holocene wet–dry transition recorded in palaeo-shorelines of Lake Turkana, northern Kenya Rift. *Earth and Planetary Science Letters* **331–332**: 322–334.
Gasse F. 2000. Hydrological changes in the African tropics since the Last Glacial Maximum. *Quaternary Science Reviews* **19**: 189–211.
Gelorini V, Ssemmanda I, Verschuren D. 2012. Validation of non-pollen palynomorphs as paleoenvironmental indicators in tropical Africa: contrasting ~200-year paleolimnological records of climate change and human impact. *Review of Palaeobotany and Palynology* **186**: 90–101.
Gichana Z, Njiru M, Raburu PO *et al*. 2015. Effects of human activities on benthic macroinvertebrate community composition and water quality in the upper catchment of the Mara River Basin, Kenya. *Lakes and Reservoirs: Research and Management* **20**: 128–137.
Gillson L, Marchant R. 2014. From myopia to clarity: sharpening the focus of ecosystem management through the lens of palaeoecology. *Trends in Ecology and Evolution* **29**: 317–325.
Gil-Romera G, Adolf C, Benito BM *et al*. 2019. Long-term fire resilience of the Ericaceous Belt, Bale Mountains, Ethiopia. *Biology Letters* **15** 20190357.
Githumbi EN. 2017. *Holocene environmental and human interactions in East Africa* PhD Thesis, University of York.
Githumbi EN, Kariuki R, Shoemaker A *et al*. 2018a. Pollen, people and place: multidisciplinary perspectives on ecosystem change at Amboseli, Kenya. *Frontiers in Earth Science* **5**: 113.
Githumbi EN, Mustaphi CJC, Yun KJ *et al*. 2018b. Late Holocene wetland transgression and 500 years of vegetation and fire variability in the semi-arid Amboseli landscape, southern Kenya. *Ambio* **47**: 682–696.
Goman MF, Ashley GM, Owen RB *et al*. 2020. A high-resolution climate history of geochemical and biological proxies from a tropical freshwater wetland located in the Kenyan Rift Valley. *Journal of African Earth Sciences* **162**.
Grimm EC, Blois JL, Giesecke T *et al*. 2018. Constituent databases and data stewards in the Neotoma Paleoecology Database: history. *growth, and new directions. Past Global Change Magazine* **26**: 64–65.
Haberyan KA, Hecky RE. 1987. The Late Pleistocene and Holocene stratigraphy and paleolimnology of Lakes Kivu and Tanganyika. *Palaeogeography, Palaeoclimatology, Palaeoecology* **61**: 169–197.
Hamilton A, Taylor D, Vogel JC. 1986. Early forest clearance and environmental degradation in south-west Uganda. *Nature* **320**: 164–167.
Hamilton AC. 1982) Upper Quaternary pollen diagrams from montane East Africa. *Environmental History of East Africa: a Study of the Quaternary*. Academic Press: London: 111–191.
Hamilton AC. 1987. Vegetation and climate of Mt Elgon during Pleistocene and Holocene. *Palaeoecology of Africa and the Surrounding Islands* **18**: 283–304.
Hawthorne D, Mitchell FJG. 2016. Identifying past fire regimes throughout the Holocene in Ireland using new and established

methods of charcoal analysis. *Quaternary Science Reviews* **137**: 45–53.
Heckmann M. 2014. Farmers, smelters and caravans: two thousand years of land use and soil erosion in North Pare, NE Tanzania. *CATENA* **113**: 187–201.
Heckmann M, Muiruri V, Boom A *et al*. 2014. Human–environment interactions in an agricultural landscape: a 1400-yr sediment and pollen record from North Pare, NE Tanzania. *Palaeogeography, Palaeoclimatology, Palaeoecology* **406**: 49–61.
Heiri O, Lotter AF, Lemcke G. 2001. Loss on ignition as a method for estimating organic and carbonate content in sediments: reproducibility and comparability of results. *Journal of Paleolimnology* **25**: 101–110.
Hoelzmann P, Gasse F, Dupont LM *et al*. 2004. Palaeoenvironmental changes in the arid and sub arid belt (Sahara–Sahel-Arabian Peninsula) from 150 kyr to present. In. *Past Climate Variability Through Europe and Africa* 219–256.
Hubbard RM, Carneiro RL, Campoe O *et al*. 2020. Contrasting water use of two Eucalyptus clones across a precipitation and temperature gradient in Brazil. *Forest Ecology and Management* 475.
Iles L. 2019. Exploring the impact of iron production on forest and woodland resources: estimating fuel consumption from slag. *STAR: Science and Technology of Archaeological Research* **5**: 179–199.
Iles L, Stump D, Heckmann M *et al*. 2018. Iron production in north Pare, Tanzania: archaeometallurgical and geoarchaeological perspectives on landscape change. *African Archaeological Review* **35**: 507–530.
Jennings DJ. 1971. *Geology of the Molo Area*. Government Press: Nairobi.–39.
Jolly D, Prentice IC, Bonnefille R *et al*. 1998. Biome reconstruction from pollen and plant macrofossil data for Africa and the Arabian peninsula at 0 and 6000 years. *Journal of Biogeography* **25**: 1007–1027.
Juggins S. 2003. *C2 User Guide: Software for Ecological and Palaeoecological Data Analysis and Visualization*. University of Newcastle, Newcastle upon Tyne; 1–73. https://www.staff.ncl.ac.uk/stephen.juggins/software/code/C2.pdf
Juggins S. 2020. *Rioja: Analysis of Quaternary Science Data*. R package version 0.9-26. https://cran.r-project.org/package=rioja
Kenya Gazette Supplement. 2012. Legal Notice No. 27 The State Corporations Act (Cap. 446). *Kenya Gazette Supplement* **27**.
Kiage LM, Liu K. 2006. Late Quaternary paleoenvironmental changes in East Africa: a review of multiproxy evidence from palynology, lake sediments, and associated records. *Progress in Physical Geography: Earth and Environment* **30**: 633–658.
Kiage LM, Liu K. 2009. Palynological evidence of climate change and land degradation in the Lake Baringo area, Kenya, East Africa, since AD 1650. *Palaeogeography, Palaeoclimatology, Palaeoecology* **279**: 60–72.
Kinjanjui JM, Karachi M, Ondimu KN. 2013. Natural regeneration and ecological recovery in Mau Forest complex, Kenya. *Open Journal of Ecology* **03**: 417–422.
Kinyanjui MJ. 2011. NDVI-based vegetation monitoring in Mau forest complex, Kenya. *African Journal of Ecology* **49**: 165–174.
Klopp JM. 2012. Deforestation and democratization: patronage, politics and forests in Kenya. *Journal of Eastern African Studies* **6**: 351–370.
Kristen I. 2009. Investigations on rainfall variability during the late Quaternary based on geochemical analyses of lake sediments from tropical and subtropical southern Africa, (PhD Thesis, Scientific Technical Report STR ; 10/01), Deutsches GeoForschungsZentrum GFZ, Potsdam. https://doi.org/10.2312/GFZ.b103-10018
Lejju BJ, Taylorl D, Robertshaw P. 2005. Late-Holocene environmental variability at Munsa archaeological site, Uganda: a multicore, multiproxy approach. *The Holocene* **15**: 1044–1061.
Lejju JB. 2009. Vegetation dynamics in western Uganda during the last 1000 years: climate change or human induced environmental degradation? *African Journal of Ecology* **47**: 21–29.
Livingstone DA. 1967. Postglacial vegetation of the Ruwenzori mountains in equatorial Africa. *Ecological Monographs* **37**: 25–52.
Loomis SE, Russell JM, Verschuren D *et al*. 2017. The tropical lapse rate steepened during the Last Glacial Maximum. *Science Advances* **3** e1600815.
Los SO, Street-Perrott FA, Loader NJ *et al*. 2019. Sensitivity of a tropical montane cloud forest to climate change, present, past and future: Mt. Marsabit, N. Kenya. *Quaternary Science Reviews* **218**: 34–48.
Malvern Instruments Ltd. 2007. *Mastersizer 2000 User Manual*. Malvern Instruments: Malvern. https://warwick.ac.uk/fac/cross_fac/sciencecity/programmes/internal/themes/am2/booking/particlesize/mastersizer_2000_essentials_manual.pdf
Marchant R, Hooghiemstra H. 2004. Rapid environmental change in African and South American tropics around 4000 years before present: a review. *Earth-Science Reviews* **66**: 217–260.
Marchant R, Richer S, Boles O *et al*. 2018. Drivers and trajectories of land cover change in East Africa: Human and environmental interactions from 6000 years ago to present. *Earth-Science Reviews* **178**: 322–378.
Marshall AR, Platts PJ, Chazdon RL *et al*. 2020. Conceptualising the global forest response to liana proliferation. *Frontiers in Forests and Global Change* **3**: 35.
McGlynn G, Mooney S, Taylor D. 2013. Palaeoecological evidence for Holocene environmental change from the Virunga volcanoes in the Albertine Rift, central Africa. *Quaternary Science Reviews* **61**: 32–46.
MEMR. 2012. *Kenya Wetlands Atlas*. Ministry of Environment and Mineral Resources (MEMR): Kenya, Nairobi. ISBN: 978-9966-21-178-1.
Merrick HV, Monaghan MC. 1984. The date of the cremated burials in Njoro River cave. *Azania: Archaeological Research in Africa* **19**: 7–11.
Msaky ES, Livingstone D, Davis OK. 2005. Paleolimnological investigations of anthropogenic environmental change in Lake Tanganyika: V. Palynological evidence for deforestation and increased erosion. *Journal of Paleolimnology* **34**: 73–83.
Mumbi CTT, Marchant R, Hooghiemstra H *et al*. 2008. Late Quaternary vegetation reconstruction from the Eastern Arc Mountains, Tanzania. *Quaternary Research* **69**: 326–341.
Mwanake RM, Gettel GM, Aho KS *et al*. 2019. Land use, not stream order, controls N2O concentration and flux in the upper Mara river basin, Kenya. *Journal of Geophysical Research. Biogeosciences* **124**: 3491–3506.
Mwangi H, Lariu P, Julich S *et al*. 2017. Characterizing the intensity and dynamics of land-use change in the Mara river basin, East. *Africa. Forests* **9**: 8.
Mwangi HM, Julich S, Patil SD *et al*. 2016a. Relative contribution of land use change and climate variability on discharge of upper Mara River, Kenya. *Journal of Hydrology: Regional Studies* **5**: 244–260.
Mwangi HM, Julich S, Patil SD *et al*. 2016b. Modelling the impact of agroforestry on hydrology of Mara River Basin in East Africa. *Hydrological Processes* **30**: 3139–3155.
Neumann FH, Scott L, Bousman CB *et al*. 2010. A Holocene sequence of vegetation change at Lake Eteza, coastal KwaZulu-Natal, South Africa. *Review of Palaeobotany and Palynology* **162**: 39–53.
Nkako F, Lambrechts C, Gachanja M, & Woodley, B. 2005. *Maasai Mau Forest Status Report 2005*.
Öberg H, Andersen TJ, Westerberg L-O *et al*. 2012. A diatom record of recent environmental change in Lake Duluti, northern Tanzania. *Journal of Paleolimnology* **48**: 401–416.
Odawa S, Seo Y. 2019. Water tower ecosystems under the influence of land cover change and population growth: focus on Mau water tower in Kenya. *Sustainability* **11**: 3524.
Ojala AEK, Francus P, Zolitschka B *et al*. 2012. Characteristics of sedimentary varve chronologies – a review. *Quaternary Science Reviews* **43**: 45–60.
Okeyo-Owuor JB. 2007. *Survey of Biodiversity Values of Enapuiyapui Swamp, Kiptunga Forest, Upper Mara River Basin, Nakuru/Molo District, Kenya*. Kisumu: Kenya.
Olago D. 2001. Vegetation changes over palaeo-time scales in Africa. *Climate Research* **17**: 105–121.
Olago DO, Street-Perrott FA, Perrott RA *et al*. 1999. Late Quaternary glacial-interglacial cycle of climatic and environmental change on Mount Kenya, Kenya. *Journal of African Earth Sciences* **29**: 593–618.
Olang L, Musula P. 2011. Land degradation of the Mau Forest Complex in Eastern Africa: a review for management and restoration

planning. In *Environmental Monitoring*, Ekundayo E (ed). In-Tech, 528.
Opiyo B, Gebregiorgis D, Cheruiyot VC *et al*. 2019. Late Quaternary paleoenvironmental changes in tropical eastern Africa revealed by multi–proxy records from the Cherangani Hills, Kenya. *Quaternary Science Reviews* **222**.
Otuoma J, Langat D, Maina J *et al*. 2012. Effect of watershed degradation on hydrological functions in the Sondu River catchment. In. IUFRO – FORNESSA Regional Congress, Nairobi, Kenya; 1–10.
Street-Perrott FA, Barker PA, Swain DL *et al*. 2007. Late Quaternary changes in ecosystems and carbon cycling on Mt. Kenya, East Africa: a landscape-ecological perspective based on multi-proxy lake-sediment influxes. *Quaternary Science Reviews* **26**: 1838–1860.
Petursson JG, Vedeld P, Sassen M. 2013. An institutional analysis of deforestation processes in protected areas: the case of the transboundary Mt. Elgon, Uganda and Kenya. *Forest Policy and Economics* **26**: 22–33.
Phelps LN, Chevalier M, Shanahan TM *et al*. 2020. Asymmetric response of forest and grassy biomes to climate variability across the African Humid Period: influenced by anthropogenic disturbance? *Ecography* **43**: 1118–1142.
Pieterse E, Parnell S, Haysom G. 2018. African dreams: locating urban infrastructure in the 2030 sustainable developmental agenda. *Area Development and Policy* **3**: 149–169.
Punwong P, Marchant R, Selby K. 2013. Holocene mangrove dynamics and environmental change in the Rufiji Delta, Tanzania. *Vegetation History and Archaeobotany* **22**: 381–396.
Quick LJ. 2013. *Late Quaternary palaeoenvironments of the southern Cape, South Africa: palynological evidence from three coastal wetlands Late Quaternary palaeoenvironments of the southern Cape, South Africa: palynological evidence from three coastal wetlands* PhD Thesis, University of Cape Town.
Republic of Kenya, 2016. The Forest Conservation and Management Act, 2016. *Kenya Gazette Supplement No. 155 (Acts No. 34)*, 677–736.
R Development Core Team. 2017. *R: A Language and Environment for Statistical Computing. R Version 3.4.0 (21 April 2017) 'You Stupid Darkness'*. R Foundation for Statistical Computing: Vienna.
Reimer PJ, Bard E, Bayliss A *et al*. 2013. IntCal13 and Marine13 radiocarbon age calibration curves 0–50,000 years cal BP. *Radiocarbon* **55**: 1869–1887.
Rey F, Gobet E, Szidat S *et al*. 2019. Radiocarbon Wiggle Matching on Laminated Sediments Delivers High-Precision Chronologies. *Radiocarbon* **61**: 265–285.
Rucina SM, Muiruri VM, Downton L *et al*. 2010. Late-Holocene savanna dynamics in the Amboseli Basin. *Kenya. The Holocene* **20**: 667–677.
Rucina SM, Muiruri VM, Kinyanjui RN *et al*. 2009. Late Quaternary vegetation and fire dynamics on Mount Kenya. *Palaeogeography, Palaeoclimatology, Palaeoecology* **283**: 1–14.
Ryner M, Holmgren K, Taylor D. 2008. A record of vegetation dynamics and lake level changes from Lake Emakat, northern Tanzania, during the last c. 1200 years. *Journal of Paleolimnology* **40**: 583–601.
Ryner MA, Bonnefille R, Holmgren K *et al*. 2006. Vegetation changes in Empakaai Crater, northern Tanzania, at 14,800–9300 cal yr BP. *Review of Palaeobotany and Palynology* **140**: 163–174.
Sang JK. 2001. The Ogiek in Mau Forest. In. *Conservation in East Africa* 35.
Sanya SM. 2008. *Forest Plantation Map Eastern Mau Sheet No. 12. 1990, Amended, January 2008*. Nairobi.
Schlachter KJ, Horn SP. 2010. Sample preparation methods and replicability in macroscopic charcoal analysis. *Journal of Paleolimnology* **44**: 701–708.
Schüler L, Hemp A, Behling H. 2014. Pollen-based temperature and precipitation inferences for the montane forest of Mt. Kilimanjaro during the last Glacial and the Holocene. *Climate of the Past Discussions* **10**: 195–234.
Schüler L, Hemp A, Zech W *et al*. 2012. Vegetation, climate and fire-dynamics in East Africa inferred from the Maundi crater pollen record from Mt Kilimanjaro during the last glacial–interglacial cycle. *Quaternary Science Reviews* **39**: 1–13.
Shanahan TM, McKay NP, Hughen KA *et al*. 2015. The time-transgressive termination of the African Humid Period. *Nature Geoscience* **8**: 140–144.
Sonzogni C, Bard E, Rostek F. 1998. Tropical sea-surface temperatures during the Last Glacial period: a view based on alkenones in Indian Ocean sediments. *Quaternary Science Reviews* **17**: 1185–1201.
Spruyt C. 2011. *Changing Concepts of Nature and Conservation Regarding Eastern Mau Forest*. Ghent.
Stager J. C., Cumming B. F. & Meeker L. D. A. 2003. 10,000-year high-resolution diatom record from Pilkington Bay, Lake Victoria, East Africa. *Quaternary Research* **59**: 172–181.
Stephens L, Fuller D, Boivin N *et al*. 2019. Archaeological assessment reveals Earth's early transformation through land use. *Science* **365**: 897–902.
Stockmarr J. 1971. Tablets with spores used in absolute pollen analysis. *Pollen et Spores* **13**: 615–621.
Swart R. 2016. *Monitoring 40 Years of Land Use Change in the Mau Forest Complex, Kenya*: a land use change driver analysis. Wageningen University: Kenya.
Syvitski JPM. 1991. *Principles, methods, and application of particle size analysis*. Cambridge University Press: Cambridge, New York, Port Chester, Melbourne, Sydney.xiii + 368 ISBN 0 521 36472 8.
Taylor DM. 1990. Late Quaternary pollen records from two Ugandan mires: evidence for environmental changes in the Rukiga Highlands of southwest Uganda. *Palaeogeography, Palaeoclimatology, Palaeoecology* **80**: 283–300.
Taylor DM, Lane PJ, Muiruri V *et al*. 2005. Mid- to late-Holocene vegetation dynamics on the Laikipia Plateau, Kenya. *The Holocene* **15**: 837–846.
Tierney JE, Russell JM. 2007. Abrupt climate change in southeast tropical Africa influenced by Indian monsoon variability and ITCZ migration. *Geophysical Research Letters* **34**: 15709–15715.
Troup RS. 1932. *Exotic Forest Trees in the British Commonwealth*. Nature Publishing: Oxford.
Urban M. A., Nelson D. M., Street-Perrott F. A., Verschuren D. & Hu F. S. 2015. A late-Quaternary perspective on atmospheric pCO2 , climate, and fire as drivers of C 4 -grass abundance. *Ecology* **96**: 642–653.
Vachula RS. 2019. A usage-based size classification scheme for sedimentary charcoal. *The Holocene* **29**: 523–527.
van der Plas GW, De Cort G, Petek-Sargeant N *et al*. 2019. Distinct phases of natural landscape dynamics and intensifying human activity in the central Kenya Rift Valley during the past 1300 years. *Quaternary Science Reviews* **218**: 91–106.
Van Zinderen Bakker EM, Coetzee JA. 1988. A review of late quaternary pollen studies in East, Central and Southern Africa. *Review of Palaeobotany and Palynology* **55**: 155–174.
Verschuren D. 2001. Reconstructing fluctuations of a shallow East African lake during the past 1800 yrs from sediment stratigraphy in a submerged crater basin. *Journal of Paleolimnology* **25**: 297–311.
Verschuren D, Laird KR, Cumming BF. 2000. Rainfall and drought in equatorial east Africa during the past 1,100 years. *Nature* **403**: 410–414.
Verschuren D, Sinninghe Damsté JS, Moernaut J *et al*. 2009. Half-precessional dynamics of monsoon rainfall near the East African Equator. *Nature* **462**: 637–641.
Vincens A. 1986. Diagramme pollinique d'un sondage Pleistocene superieur – Holocene du Lac Bogoria (Kenya). *Review of Palaeobotany and Palynology* **47**: 169–192.
Vincens A, Lézine AM, Buchet G *et al*. 2007. African pollen database inventory of tree and shrub pollen types. *Review of Palaeobotany and Palynology* **145**: 135–141.
Walker M, Head MJ, Lowe J *et al*. 2019. Subdividing the Holocene Series/Epoch: formalization of stages/ages and subseries/subepochs, and designation of GSSPs and auxiliary stratotypes. *Journal of Quaternary Science* **34**: 173–186.
Were KO, Dick ØB, Singh BR. 2013. Remotely sensing the spatial and temporal land cover changes in Eastern Mau forest reserve and Lake Nakuru drainage basin, Kenya. *Applied Geography* **41**: 75–86.
Were O, Singh BR, Dick ØB. 2015. Effects of land cover changes on soil organic carbon and total nitrogen stocks in the Eastern Mau Forest Reserve, Kenya Kennedy. In *Sustainable Intensification to Advance Food Security and Enhance Climate Resilience in Africa*,

Lal R, Singh BR, Mwaseba DL, Kraybill D, Hansen DO, Eik LO (eds). Springer International Publishing: Cham; 407–424.

Whitlock C, Higuera PE, McWethy DB *et al*. 2010. Paleoecological perspectives on fire ecology: revisiting the fire-regime concept. *Open Ecology Journal* **3**: 6–23.

Williams JW, Grimm EC, Blois JL *et al*. 2018. The Neotoma Paleoecology Database, a multiproxy, international, community-curated data resource. *Quaternary Research* **89**: 156–177.

Williams LAJ. 1991. *Geology of the Mau Area*. Mines and Geological Department: Nairobi.

Wolff C. 2011. East African monsoon variability since the last glacial. *Potsdam. Scientific Technical Report STR12/17*.

Wood PJ. 1965. A note on forestry on Kilimanjaro. *Tanganyika Notes and Records* **64**: 111–114.

Wright D. K.. 2005. Environment, Chronology and Resource Exploitation of the Pastoral Neolithic in Tsavo, Kenya. University of Illinois